JACS
JOURNAL OF THE AMERICAN CHEMICAL SOCIETY

Article

pubs.acs.org/JACS

Pyro-Borates, *Spiro*-Borates, and Boroxinates of BINOL—Assembly, Structures, and Reactivity

Gang Hu,[†] Anil K. Gupta,[†] Li Huang,[†] Wenjun Zhao,[†] Xiaopeng Yin,[†] Wynter E. G. Osminski,[†] Rui H. Huang,[†] William D. Wulff,*[,†] Joseph A. Izzo,[‡] and Mathew J. Vetticatt*[,‡]

[†]Department of Chemistry, Michigan State University, East Lansing, Michigan 48824, United States

[‡]Department of Chemistry, Binghamton University, Binghamton, New York 13902, United States

Supporting Information

ABSTRACT: VANOL and VAPOL ligands are known to react with three equivalents of $B(OPh)_3$ to form a catalytic species that contains a boroxinate core with three boron atoms, and these have proven to be effective catalysts for a number of reactions. However, it was not known whether the closely related BINOL ligand will likewise form a boroxinate species. It had simply been observed that mixtures of BINOL and $B(OPh)_3$ were very poor catalysts compared to the same mixtures with VANOL or VAPOL. Borate esters of BINOL have been investigated as chiral catalysts, and these include *meso*-borates, *spiro*-borates, and *diborabicyclo*-borate esters. Borate esters are often in equilibrium, and their structures can be determined by stoichiometry and/or thermodynamics, especially in the presence of a base. The present study examines the structures of borate esters of BINOL that are produced with different stoichiometric combinations of BINOL with $B(OPh)_3$ in the presence and absence of a base. Depending on conditions, *pyro*-borates, *spiro*-borates, and boroxinate species can be generated and their effectiveness in a catalytic asymmetric aziridination was evaluated. The finding is that BINOL borate species are not necessarily inferior catalysts to those of VANOL and VAPOL but that, under the conditions, BINOL forms two different catalytic species (a boroxinate and a *spiro*-borate) that give opposite asymmetric inductions. However, many BINOL derivatives with substitutents in the 3- and 3′-positions gave only the boroxinate species and the 3,3′-Ph_2BINOL ligand gave a boroxinate catalyst that gives excellent inductions in the aziridination reaction. BINOL derivatives with larger groups in the 3,3′-position will not form either *spiro*-borates or boroxinate species and thus are not effective catalysts at all.

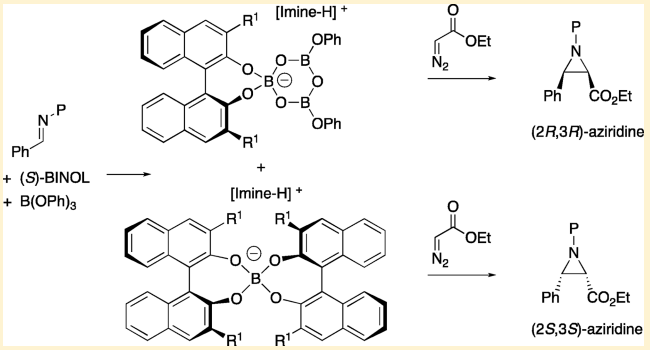

1. INTRODUCTION

BINOL **1** is a C_2-symmetrical biaryl ligand that has been widely used in a variety of asymmetric reactions.[1] The lack of ability of BINOL **1a** to render high asymmetric inductions in many systems has been related to the topological fact that its largest chiral pocket (naphthalene rings) and its active site (hydroxy groups) are on opposite sides of the axis of chirality. The traditional solution to this limitation is to employ BINOL derivatives which have substituents in the 3- and 3′-positions, thus enhancing the chiral pocket around the active site (Figure 1). This approach has led to the generation of a large family of BINOL ligands which, as a whole, have made BINOL and its derivatives one of the most important ligand types in asymmetric catalysis.[2] Our approach to this problem has been to reorient the direction of the naphthalene rings such that they are projected in a vaulted fashion around the active site, and prototypical examples of this family of vaulted biaryls are *iso*-VAPOL **2**, VANOL **3**, and VAPOL **4**. These vaulted biaryl ligands have been demonstrated to be useful in a variety of useful asymmetric reactions including Diels–Alder reactions,[3,4] Mannich reactions,[5] Baeyer–Villiger reactions,[6] heteroatom Diels–Alder reactions,[7] the amidation[8] and imidation[9] of imines, the asymmetric reduction of imines,[10] desymmetrization of aziridines,[11a−e] desymmetrization of diesters,[11f] the Petasis reaction,[12] the hydroarylation of alkenes,[13] *cis*-aziridination of imines[14,15] and *trans*-aziridination of imines,[16] benzoyloxylation of aryloxindoles,[17] the 2-aza-Cope rearrangement,[18] the Ugi reaction,[21] aza-Darzens reaction,[19] hydrogenation of alkenes,[20] propargylation of ketones,[22] chorination and Michael reactions of oxindoles,[23] hydroacylation of alkenes,[24] pinacol rearrangement,[25a] α-imino rearrangement,[25b] reduction of aminals,[26] Michael addition of alkynes,[27a] chromene functionalization,[27b] carbonylative spirolactonization of enallenols,[27c] and controlled switching in a foldamer.[27d] More recently, we have reported the preparation of a number of derivatives of these vaulted ligands and these new ligand types have been evaluated in the catalytic asymmetric aziridination reaction,[15] Diels–Alder reactions,[4] Ugi reactions,[21] and enantioselective protonation.[27e]

Received: March 7, 2017
Published: June 28, 2017

DOI: 10.1021/jacs.7b02317
J. Am. Chem. Soc. 2017, 139, 10267−10285

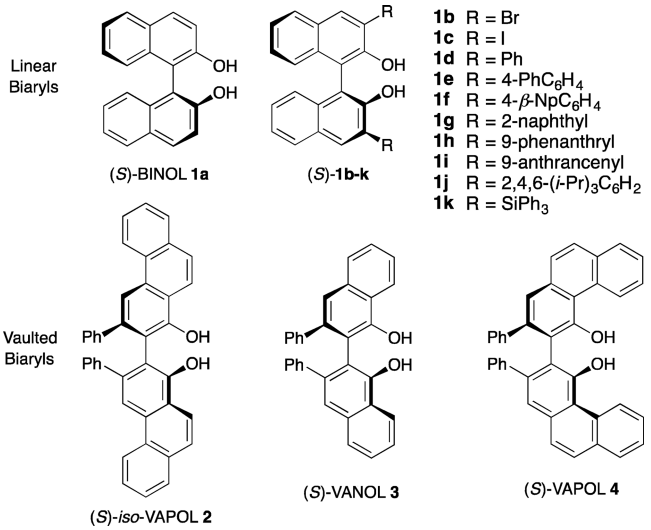

Figure 1. Linear and vaulted biaryls.

The aziridination of imines with diazo compounds is arguably the most successful reaction to date that is catalyzed by a VANOL or VAPOL derived catalyst.[14−16] These aziridination catalysts were originally prepared by heating the ligand with 3 equiv of $B(OPh)_3$ and then removing all volatiles under a vacuum, as indicated by the procedure in Table 1.[14a] Data that compare the relative effectiveness of BINOL, VANOL, and VAPOL with imines with different protecting groups on the nitrogen have been collected from the literature and presented in Table 1. In each case, it can be seen that the BINOL derived catalyst gives far inferior asymmetric inductions when compared to the catalyst generated from either VANOL or VAPOL. This observation is consistent with the hypothesis that motivated the design and synthesis of the vaulted biaryl ligands: BINOL has a smaller chiral pocket around the active site than VANOL or VAPOL. Also consistent with this hypothesis is the increase of asymmetric induction for the aziridine **7a** from 13% ee to 54% ee when the BINOL catalyst has 3- and 3′-substituents (Table 1, entries 1 vs 2).[28] Not consistent with this hypothesis is the fact that for all three imines shown in Table 1 the catalysts derived from VANOL and VAPOL give nearly identical asymmetric inductions. It would have been expected that the VAPOL catalyst would have given higher asymmetric inductions than VANOL, since the active site is contained within a deeper chiral pocket in VAPOL than in VANOL.[29] Any attempt to correlate the effectiveness of these ligands and the size of the chiral pocket around the active site of course must presuppose that the structure of the catalyst is the same for all of the ligands. Thus, while we have recently gained some information concerning the structure of the boron based catalysts[14d] generated from VANOL and VAPOL and $B(OPh)_3$, not nearly as much is known about BINOL borates. The purpose of the present work is to take a closer look at the structure and reactivity of various BINOL borate esters that are generated upon interaction of BINOL and $B(OPh)_3$. The findings are that the supposition that BINOL, VANOL, and VAPOL give the same type of catalyst is not correct and, furthermore, that BINOL gives a mixture of two species under conditions where VANOL and VAPOL give a single borate species. Computational analysis of the aziridination reactions catalyzed with the different BINOL borate species supports the experimental observations that the low asymmetric inductions with BINOL derived borate catalysts (Table 1) are due to the presence of two catalyst species that give opposite enantiomers.

Table 1. BINOL Catalysts for the Catalytic Asymmetric Aziridination Reaction

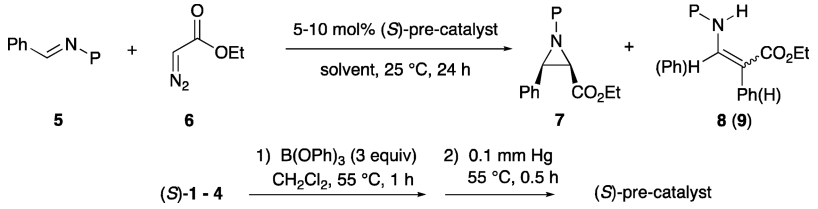

series	P	ligand	mol% catalyst	solvent	% yield *cis*-**7** [a]	cis/trans **7** [b]	% ee **7** [c]	% yield **8** + **9** [b]
a	Benzhydryl (Bh)	BINOL **1a** [d]	10	toluene	66	>50:1	13	17
		BINOL **1g** [e]	10	toluene	55	99:1	54	nd
		VANOL **3**	5	toluene	87	>50:1	89	<1
		VAPOL **4** [f]	5	toluene	82	>33:1	94	2
b	MEDAM	BINOL **1a** [g]	5	toluene	72	17:1	38	24
		VANOL **3**	5	toluene	98	50:1	97	2
		VAPOL **4** [h]	5	toluene	98	>33:1	99	2
c	BUDAM	BINOL **1a** [h]	10	CH_2Cl_2	71	nd	67	nd
		VANOL **3**	5	toluene	98	>50:1	96	<2
		VAPOL **4** [h]	10	CH_2Cl_2	96	>50:1	99	<2

[a]Isolated yield after silica gel chromatography. [b]Determined from the ^1H NMR spectrum of the crude reaction mixture. [c]Determined by chiral HPLC on purified *cis*-**7**. [d]See Table 2, entry 9. [e]Reference 28. [f]Precatalyst prepared by method B in Table 2; ref 14a. [g]Precatalyst made from 4 equiv of $B(OPh)_3$ in toluene at 85 °C and then removal of volatiles; ref 14c. [h]Reference 14b.

DOI: 10.1021/jacs.7b02317
J. Am. Chem. Soc. 2017, 139, 10267−10285

Scheme 1

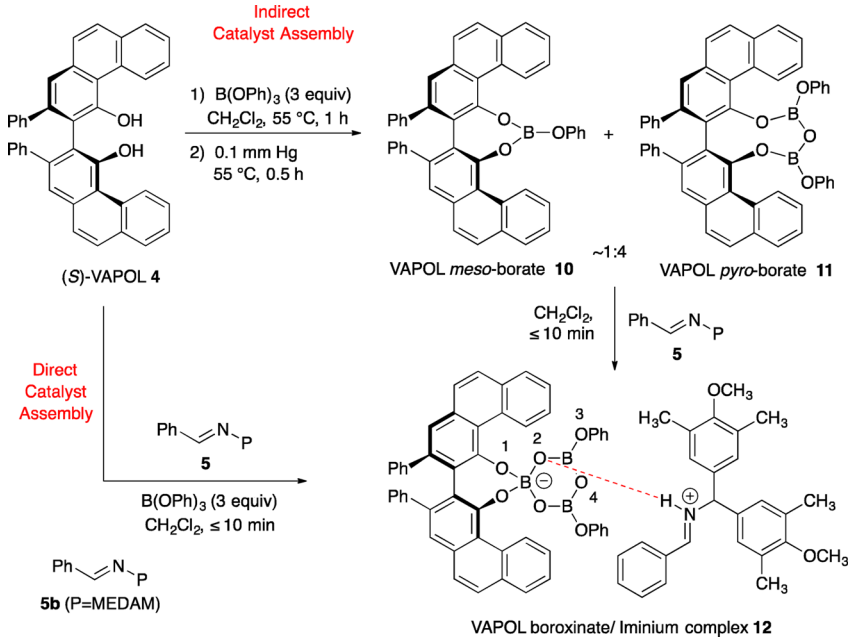

Scheme 2

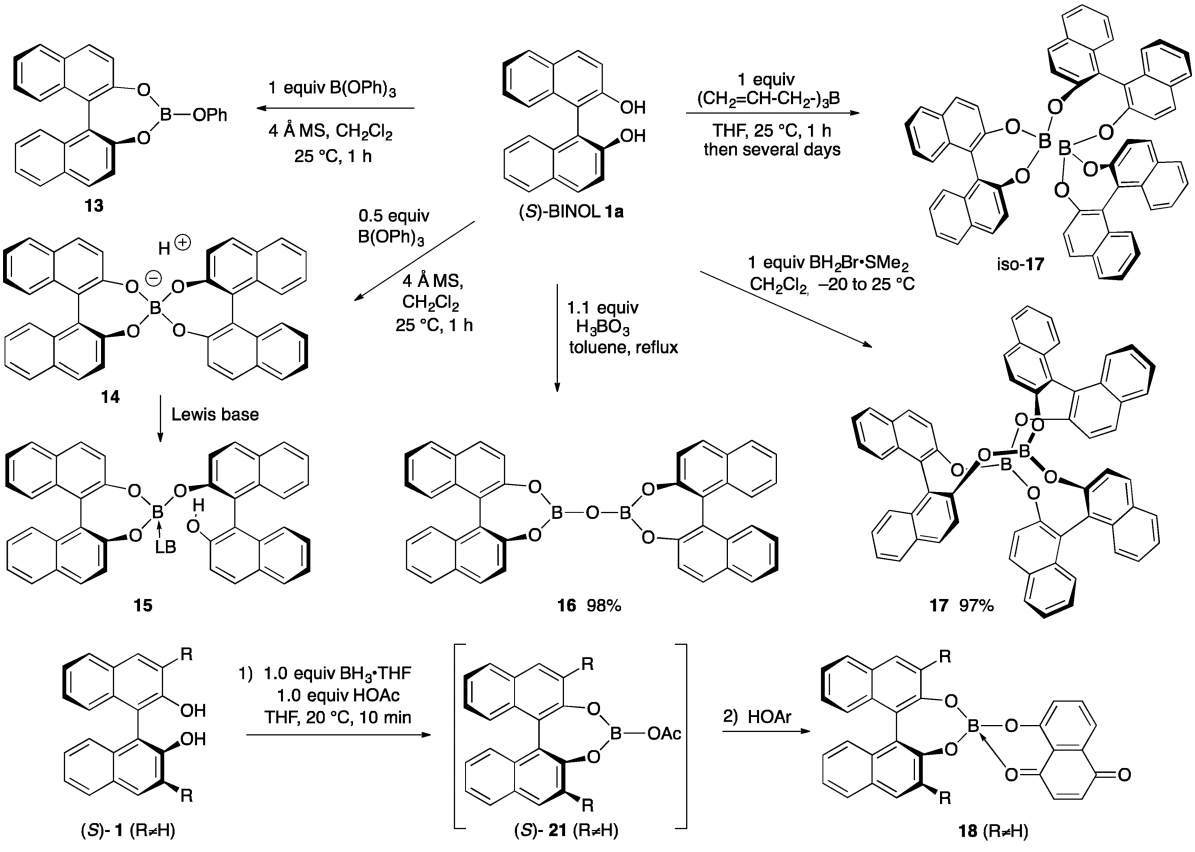

2. BACKGROUND

VANOL and VAPOL Catalysts and Precatalysts. The procedure involving heating the VAPOL ligand with 3 equiv of $B(OPh)_3$ as indicated in Scheme 1 (Indirect Catalyst Assembly) produces two species, and the ^1H NMR, ^{11}B NMR, and mass spectroscopic analysis of this mixture support the assignment of the *meso*-borate **10** and the *pyro*-borate **11** as the components of this mixture.[14f] The ratio of these two species varies with the method of preparation, but typically the *pyro*-borate **11** is favored by a factor of ~4. The VAPOL *pyro*-borate was originally tentatively assigned as the linear isomer,[14a] but more recent studies have led to its reassignment as the cyclic isomer **11**.[14f] Neither the *meso*-borate **10** nor the *pyro*-borate **11** are catalysts in the aziridination reaction, and the

DOI: 10.1021/jacs.7b02317
J. Am. Chem. Soc. 2017, 139, 10267–10285

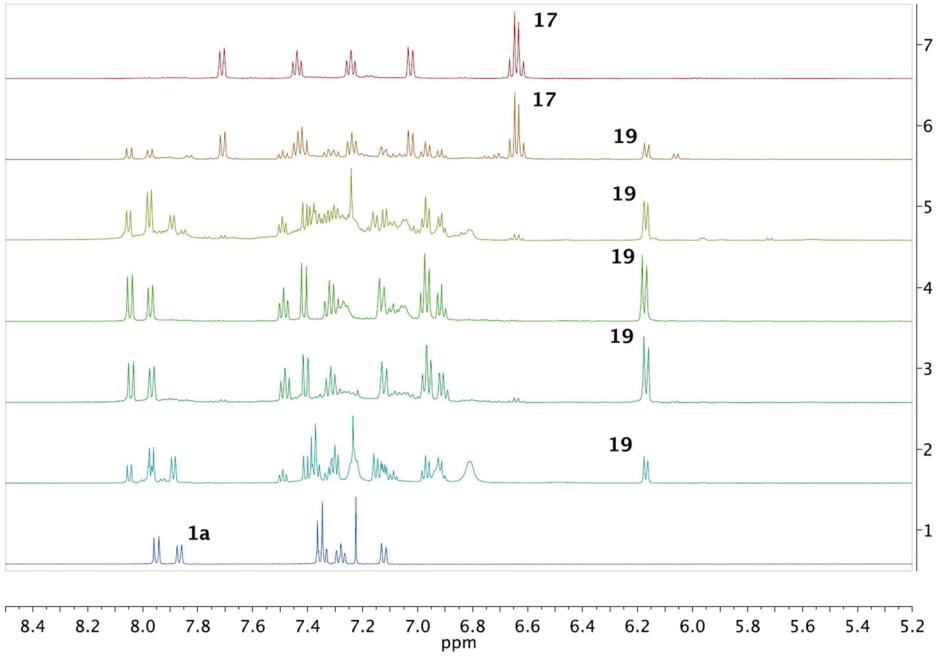

Figure 2. ^{1}H NMR of BINOL–borate complexes. Unless otherwise specified, all NMR spectra were performed in $CDCl_3$. (1) Pure BINOL in $CDCl_3$. (2) BINOL and $B(OPh)_3$ (1:1) were combined in $CDCl_3$ for 10 min. (3) BINOL pyroborate **19** prepared by heating a mixture of BINOL, $BH_3{\cdot}Me_2S$, phenol, and H_2O (1:2:3:1) at 55 °C. (4) BINOL pyroborate **19** prepared by heating a mixture of BINOL and $B(OPh)_3$ (1:3) at 100 °C. (5) BINOL pyroborate **19** prepared by heating a mixture of BINOL, $BH_3{\cdot}Me_2S$, phenol, and H_2O (1:3:2:3) at 80 °C. (6) A mixture of BINOL, $BH_3{\cdot}Me_2S$, and phenol (1:1:1) was heated at 50 °C. (7) Kaufmann's propeller prepared by heating a mixture of BINOL and $BH_3{\cdot}Me_2S$ (1:1) at 80 °C.

mixture of these two species is in fact a precatalyst. Treatment of the mixture of **10** and **11** with an imine leads to the generation of the boroxinate **12** which is the active catalyst and which consists of an ion pair comprised of a chiral boroxinate anion and a protonated iminium.[14d] The complex **12** has been fully characterized including X-ray analysis, and crystals of this complex will catalyze the aziridination reaction.[14d] A complex array of noncovalent interactions between the catalyst and the substrate in **12** was revealed by the X-ray diffraction analysis.[14d] We have subsequently found that it is not necessary to prepare the precatalyst in order to generate the VAPOL boroxinate **12** (BOROX catalyst). The covalent assembly of complex **12** can be induced in a few minutes at room temperature upon mixing VAPOL, $B(OPh)_3$, and an imine (Direct Catalyst Assembly), conditions under which there is no reaction between VAPOL and $B(OPh)_3$.[14d] It is also interesting to note that the formation of the three B–O–B bonds in the boroxinate core of complex **12** from $B(OPh)_3$ requires 3 equiv of H_2O. This is consistent with the fact that the use of purified $B(OPh)_3$ will not lead to the generation of the boroxinate catalyst **12** unless 3 equiv of H_2O are added. Nearly all of the commercial samples of $B(OPh)_3$ that we have examined over the years will generate active catalysts, suggesting that these samples contain at least three OH equivalents resulting from partial hydrolysis.[14d] In addition to aziridination reactions,[14−16] BOROX catalysts of the type **12** have been shown to be involved in 2-aza-Cope rearrangements,[18] a catalytic asymmetric Ugi reaction,[21] and presumably heteroatom Diels–Alder reactions[7] as well.

Known Borate Esters of BINOL. The most common structural types reported for borate esters of BINOL are shown in Scheme 2.[30] The reaction of BINOL with 1 equiv of $B(OPh)_3$ has been reported to give a compound for which the most probable structure was suggested to be the *meso*-borate **13** but other possible structures could not be excluded.[31a,32] This material has been examined as a catalyst for Mannich and heteroatom Diels–Alder reactions of imines,[31] the heteroatom Diels–Alder reactions of aldehydes,[33] Diels–Alder reactions,[34] and aldol reactions.[35] The reaction of BINOL with 0.5 equiv of $B(OPh)_3$ or $B(OMe)_3$ has been reported to give the *spiro*-borate **14**. Structure **14** has been suggested to function as a chiral Lewis acid catalyst for a number of reactions including Mannich reactions,[31h,36] heteroatom Diels–Alder reactions of imines,[31h,37] and Pictet–Spengler reaction.[38] The catalytic function of **14** was proposed to behave as a chiral Lewis acid where interaction with a Lewis base disrupts one of the boron–oxygen bonds to give the Lewis acid–Lewis base complex **15**.[31h,38a] There has been considerable interest in the chiral anion unit in **14**, and the sources of interest include use as a vehicle for the resolution of BINOL,[39] for examining chiral recognition in contact ion pairs,[40a] as a structural unit in solution and in the solid state,[40b,c] as a chiral shift reagent,[41] and also as a chiral counterion catalyst in aziridination reactions,[42] in Friedel–Crafts reactions,[43a] in hydrogenations,[43b] in ring-opening of *meso*-aziridiniums,[43a] and in the ring-opening of *meso*-epoxides.[44] The intriguing propeller-like structure **17** was discovered by Kaufmann and Boese when they reacted BINOL with 1 equiv of $BH_2Br{\cdot}SMe_2$ complex.[34] This bis-triaryl borate was isolated in nearly quantitative yield and contains a [6.6.6]-propellane unit composed of three units of BINOL and two borons and was characterized by X-ray diffraction. This complex has been shown to give high asymmetric inductions in Diels–Alder reactions as a chiral Lewis acid; however, as might be expected, the rates of reaction are quite slow.[34,45] An isomer of **17** has been reported by Liu and co-workers (Scheme 2).[46] This compound iso-**17** was also found to be composed of three units of BINOL and two borons and was characterized by NMR spectroscopy. It was reported to be formed from the decomposition of the allyl-boronate (not

DOI: 10.1021/jacs.7b02317
J. Am. Chem. Soc. 2017, 139, 10267–10285

shown) that was generated from the reaction of BINOL **1a** with triallylborane upon standing for several days. Another interesting structure that has been reported is the *pyro*-borate **16**, which was reported to form upon refluxing BINOL in toluene with 1.1 equiv of boric acid.[47] The *pyro*-borate **16** was characterized by combustion analysis and by IR spectroscopy and was used in the resolution of BINOL. The veracity of the structural assignment of **16** has been called into question, as it has been reported that heating BINOL and boric acid in refluxing benzene gives rise to the Kaufmann's propeller **17**.[39a] Perhaps the earliest and most widely used class of triaryl borates are those that have internal chelation of the boron to a quinone moiety. Kelly first prepared borates of the type **18** in 1986 for the purpose of effecting asymmetric Diels–Alder reactions on naphthoquinones.[4,48,49]

3. RESULTS AND DISCUSSION

Borate Esters from a 1:1 Ratio of BINOL and $B(OPh)_3$. While the reaction of VAPOL **4** with 3 equiv of $B(OPh)_3$ gives a 4:1 mixture of *pyro*-borate **11** to *meso*-borate **10** (Scheme 1), a simple change in stoichiometry to a 1:1 mixture of VAPOL and $B(OPh)_3$ gives a 17:1 mixture in favor of the *meso*-borate **10**.[14f] Similarly, a 1:1 mixture of VANOL **3** and $B(OPh)_3$ gives a 10:1 mixture in favor of the *meso*-borate.[14f] In contrast, in the present work, we find that a 1:1 mixture of BINOL and $B(OPh)_3$ gives predominately the *pyro*-borate **19** (Figure 2, entry 2, and Scheme 3). Essentially, all of the BINOL is accounted for in **19** and unreacted BINOL. The assignment of the structure of **19** will be discussed later (Scheme 6), and the complete assignment of all of the protons of **19** can be found in the Supporting Information. The spectra in entry 2 of Figure 2 were taken on a sample generated by combining BINOL and 1 equiv of $B(OPh)_3$ in $CDCl_3$ for 10 min. Essentially, the same spectrum was observed when BINOL and 1 equiv of $B(OPh)_3$ were allowed to react in CD_2Cl_2 for 1 h in the presence of 4 Å molecular sieves according to the original report[31a,32] (see the Supporting Information for ^1H and ^{11}B NMR spectra). If the $B(OPh)_3$ is purified and stored in a drybox, essentially no reaction will occur with BINOL (this was done with a 2:1 mixture of BINOL and $B(OPh)_3$; see Figure 7a, entry 2). This lack of reactivity with purified $B(OPh)_3$ has been previously observed with VANOL or VAPOL.[14d] This is in contrast to the reaction of BINOL with commercial $B(OPh)_3$ shown in entry 2 of Figure 2. An equivalent of H_2O is needed to create the B–O–B linkage, and it is our experience that most commercial $B(OPh)_3$ samples contain 20–30% phenol as a result of partial hydrolysis.[14d] Cleaner spectra for the *pyro*-borate **19** could be obtained by heating BINOL with 2 or 3 equiv of a boron source ($B(OPh)_3$ or $BH_3{\cdot}SMe_2$ + phenol), as indicated in entries 3 and 4 in Figure 2.

Given the failure to prepare the *meso*-borate ester **13** from BINOL and $B(OPh)_3$, other approaches were attempted. The first was to heat a 1:1:1 mixture of BINOL, $BH_3{\cdot}SMe_2$, and phenol at 50 °C, and the ^1H NMR spectrum of the resulting mixture is shown in entry 6 of Figure 2. The BINOL is completely consumed, but the major product is Kaufmann's propeller **17** along with the *pyro*-borate **19** (doublet, δ = 6.17 ppm) as the second major product (the mole ratio of **17**:**19** = 53:47). Other minor products were observed, but their identity could not be determined. A clean spectrum of Kaufmann's propeller **17** was generated by heating a 1:1 mixture of BINOL and $BH_3{\cdot}SMe_2$ (Figure 2, entry 7).

Scheme 3

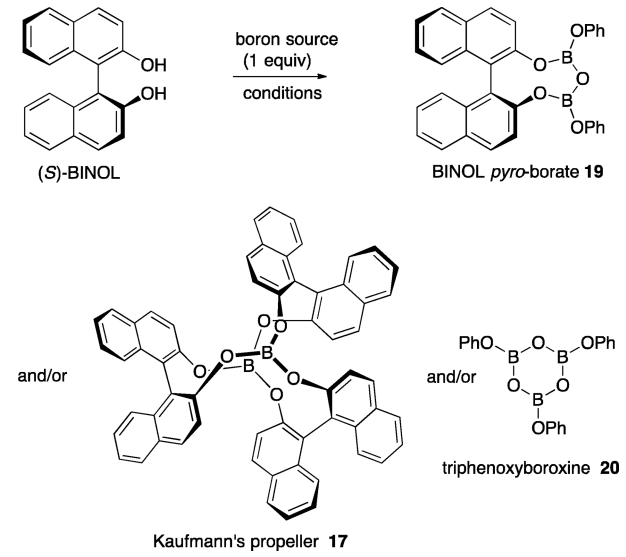

A second strategy for access to the *meso*-borate **13** is shown in Scheme 4 and involves the method of Kelly.[48,49] Kelly had

Scheme 4

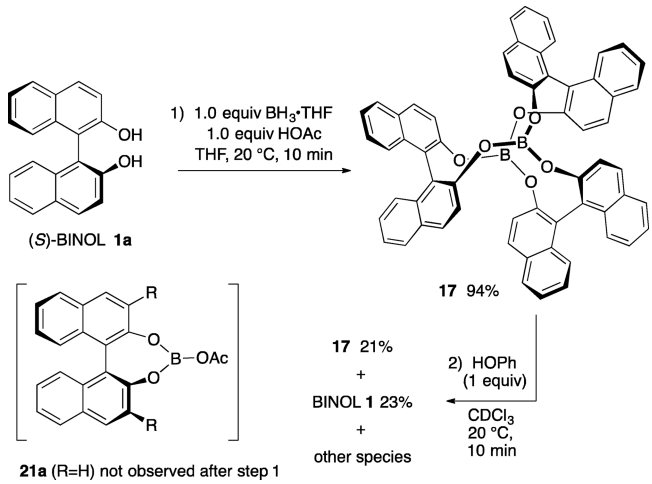

found that acetic acid will accelerate the reaction of BINOL derivatives with borane–THF complex and thus would generate the intermediate borate mixed anhydrides of the type **21** to activate the boron for reaction with 8-hydroxynaphthoquinone species to give borate esters of the type **18** shown in Scheme 2. Following Kelly's procedure, BINOL **1a** was allowed to react with 1 equiv of $BH_3{\cdot}THF$ complex and 1 equiv of acetic acid in THF at 20 °C for 10 min, and then, all volatiles were removed and the residue taken up in $CDCl_3$. However, the ^1H NMR spectrum revealed that Kaufmann's propeller had formed in 94% yield (Scheme 4). Addition of 1 equiv of phenol to the NMR tube revealed that, after 10 min at room temperature, much of Kaufmann's propeller had exchanged into a number of species with the liberation of 23% of the BINOL. A complex mixture of minor species was observed that included a 2% yield of the *pyro*-borate **19**. Kaufmann's propeller remained the major borate ester species that contains a BINOL ligand. In light of the failure to in situ generate the acetoxy borate ester derivative **21a** (R = H),

DOI: 10.1021/jacs.7b02317
J. Am. Chem. Soc. 2017, 139, 10267–10285

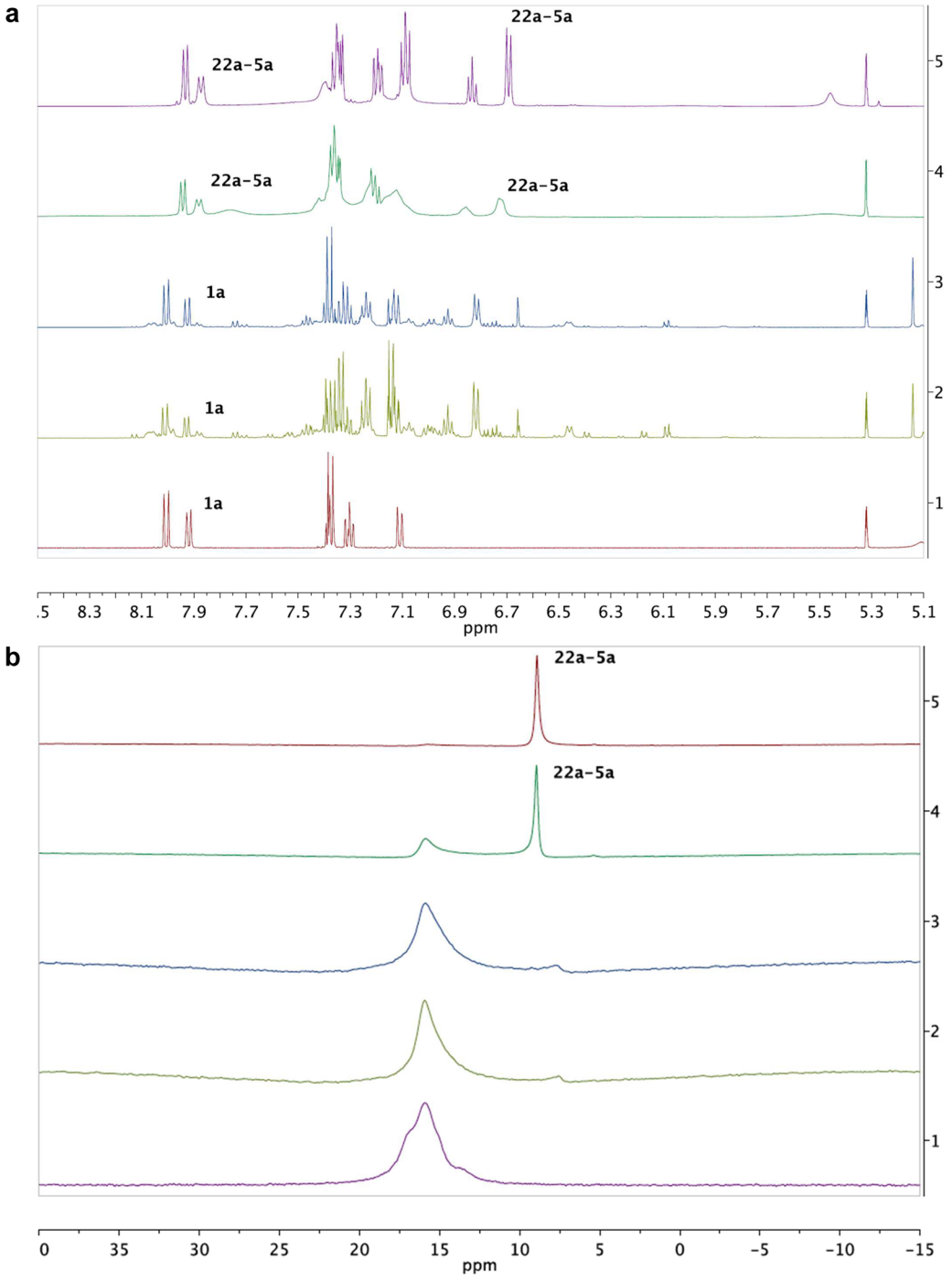

Figure 3. (a) ^{1}H NMR of BINOL–*spiro*-borate complex **22a–5a**. Unless otherwise specified, all NMR spectra were performed in CD_2Cl_2. (1) Pure BINOL. (2) A mixture of BINOL and $B(OPh)_3$ (1:1) was allowed to react in CD_2Cl_2 for 1 h at 25 °C over 4 Å molecular sieves. (3) A mixture of BINOL and $B(OPh)_3$ (2:1) was allowed to react in CD_2Cl_2 for 1 h at 25 °C over 4 Å molecular sieves (4) One equivalent of imine **5a** added to entry 2. (5) One equivalent of imine **5a** added to entry 3. (b) ^{11}B NMR of BINOL–*spiro*-borate complex **22a–5a**. Unless otherwise specified, all NMR spectra were performed in CD_2Cl_2. (1) Pure $B(OPh)_3$. (2) A mixture of BINOL and $B(OPh)_3$ (1:1) was allowed to react in CD_2Cl_2 for 1 h at 25 °C over 4 Å molecular sieves. (3) A mixture of BINOL and $B(OPh)_3$ (2:1) was allowed to react in CD_2Cl_2 for 1 h at 25 °C over 4 Å molecular sieves. (4) One equivalent of imine **5a** added to entry 2. (5) One equivalent of imine **5a** added to entry 3.

it should be pointed out that the successful preparation of **18** by Kelly was with a 3,3′-disubstituted BINOL derivative (**1d**, R = Ph), a class of compounds that are known not to form Kaufmann's trimer.[34]

Borate Esters from a 1:0.5 Ratio of BINOL and $B(OPh)_3$. The reaction of $B(OPh)_3$ with 2 equiv of BINOL was reported by Yamamoto to give the *spiro*-borate **14** simply by stirring the two in CD_2Cl_2 over 4 Å molecular sieves for 1 h at room temperature (Scheme 2).[31h,51] We have repeated this reaction and examined the ^{1}H and ^{11}B NMR spectra which are presented in Figure 3. The ^{1}H NMR spectrum (Figure 3a, entry 3) reveals that unreacted BINOL is present in substantial amounts (47%) along with the *pyro*-borate **19** (6%).[50] A small amount of a number of other species are present, as indicated

DOI: 10.1021/jacs.7b02317
J. Am. Chem. Soc. 2017, 139, 10267–10285

Scheme 5

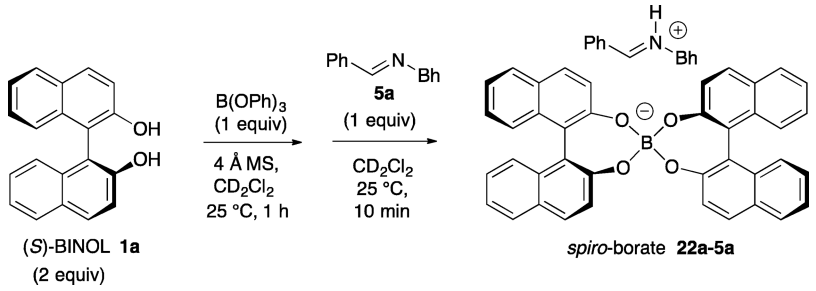

by the ^{1}H NMR spectrum, but these have not been identified. The ^{1}H NMR spectra of a 1:1 and 2:1 mixture of BINOL and $B(OPh)_3$ are quite similar to unreacted BINOL as the major species present (37% vs 47%, respectively, Figure 3a, entries 2 and 3). Comparing Figure 3a, entry 2, and Figure 2, entry 2, the amount of *pyro*-borate **19** that is produced varies quite a bit and is dependent on the batch of $B(OPh)_3$ that is used.

A dramatic simplification of the spectra is observed when the mixtures of BINOL and $B(OPh)_3$ are treated with the imine **5a**. When the mixture of 2 equiv of BINOL and 1 equiv of $B(OPh)_3$ (Figure 3a, entry 3) is treated with 1 equiv of the imine **5a** (Figure 3a, entry 5), the complex mixture of compounds is converted cleanly into a single compound which is identified as the *spiro*-borate **22a−5a** (Scheme 5). The same clean formation of **22a−5a** is observed whether BINOL and $B(OPh)_3$ are first mixed with 4 Å MS for 1 h followed by imine **5a** or whether BINOL, $B(OPh)_3$, and imine **5a** are immediately mixed and allowed to react only within the time that it takes to load an NMR tube and take the ^{1}H NMR and ^{11}B NMR spectra (Figure 3a, entry 5, and Figure 3b, entry 5). This compound is assigned as the ion pair **22a−5a** comprised of a *spiro*-borate anion and the protonated form of the imine **5a** and is formed in 94% yield.[50] The ^{1}H NMR spectrum in entry 5 of Figure 3a is of a 3:1 mixture of phenol to **22a−5a**, as would be expected from the reaction of a 2:1:1 mixture of BINOL, imine **5a**, and $B(OPh)_3$. The four-coordinate anionic borate unit in **22a−5a** displays a characteristic sharp absorption at δ = 8.9 ppm in the ^{11}B NMR spectrum (Figure 3b, entry 5) and reveals the complete disappearance of the broad three-coordinate borate absorption at δ = 16 ppm, consistent with the formation of **22a−5a** in very high yield. The *spiro*-borate **22a−5a** is also formed (75% yield)[50] when 1 equiv of imine **5a** is added to a 1:1 mixture of BINOL and $B(OPh)_3$, but in this case, the ^{11}B NMR spectrum indicates the presence of both the three- and four-coordinate borons in a 1.0:1.2 ratio (Figure 3b, entry 4). Taken together with the fact that the ^{1}H NMR reveals (Figure 3a, entry 4) that BINOL is completely consumed when the imine is added, this is consistent with conversion of all of the BINOL and half of the $B(OPh)_3$ to the complex **22a−5a**. Thus, the treatment of $B(OPh)_3$ with either 1 or 2 equiv of BINOL leads only to partial conversion to a complex mixture of compounds. However, treatment of either of these mixtures with an imine gives clean conversion to a chiral *spiro*-borate.

Support for the structure **22a−5a** containing a *spiro*-borate anion and an iminium cation comes from the work of Yamamoto and co-workers who have previously studied heteroatom Diels−Alder and Mannich reactions of imines mediated by a stoichiometric amount of a catalyst prepared from 2 equiv of BINOL and 1 equiv of $B(OPh)_3$.[31h] They were able to isolate and determine the X-ray structure of the complex **22a−5d**, although no other spectral data for **22a−5d** was presented (Figure 4).[31h] This complex consists of the *spiro*-

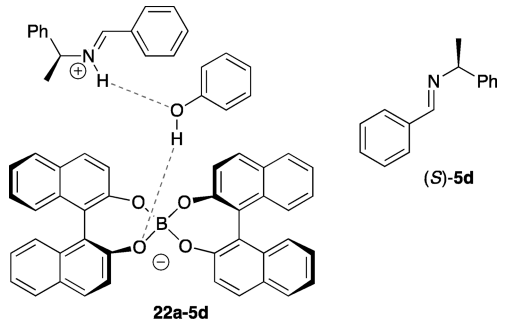

Figure 4. Schematic drawing of Yamamoto's crystal structure of **22a−5d** from (*S*)-BINOL, $B(OPh)_3$, and imine (*S*)-**5d**.

borate anion, a molecule of phenol, and the protonated form of imine (*S*)-**5d**. There is no direct H-bonding between the protonated iminium and the *spiro*-borate anion, but rather, the protonated iminium is H-bonded to the phenol, which in turn is H-bonded to the *spiro*-borate anion. This crystal was of the mismatched pair of (*S*)-BINOL and (*S*)-**5d**, and perhaps, in the matched pair, noncovalent contacts between the (*S*)-BINOL core and protonated (*R*)-**5d** would be more favorable. While studying the NMR spectra of the complex **22a−5a** containing an achiral imine (Figure 5), yellow crystals were serendipitously formed in the NMR tube and thus the opportunity to determine the crystal structure of the ion pair **22a−5a** (Figure 5) presented itself. It was hoped that noncovalent interactions between the *spiro*-borate core and the iminium could be found in **22a−5a**, since the imine **5a** from which it is derived is not chiral.

It was found that complex **22a−5a** also crystallized with a molecule of phenol, but an X-ray diffraction analysis of these crystals revealed that the noncovalent interactions present in complex **22a−5a** (Figure 5) are much different than those in Yamamoto's complex **22a−5d** (Figure 4). There are several direct interactions between the iminium ion and the *spiro*-borate core. The iminium proton is directly H-bonded to the *spiro*-borate anion with a biased bifurcated H-bond that spans two of the oxygens of the *spiro*-borate (Figure 5, d_2 and d_3). The phenol unit is also H-bonded to the *spiro*-borate core but to the opposite side of the anion to which the iminium is H-bonded. Additional secondary interactions between the iminium substrate and the *spiro*-borate catalyst include two CH−π interactions between the edges of the phenyl rings of the iminium and the faces of the naphthalene rings of the *spiro*-borate anion (Figure 5, d_1 and d_4). As a result of these interactions, the benzylidene iminium plane (with the coplanar

DOI: 10.1021/jacs.7b02317
J. Am. Chem. Soc. 2017, 139, 10267−10285

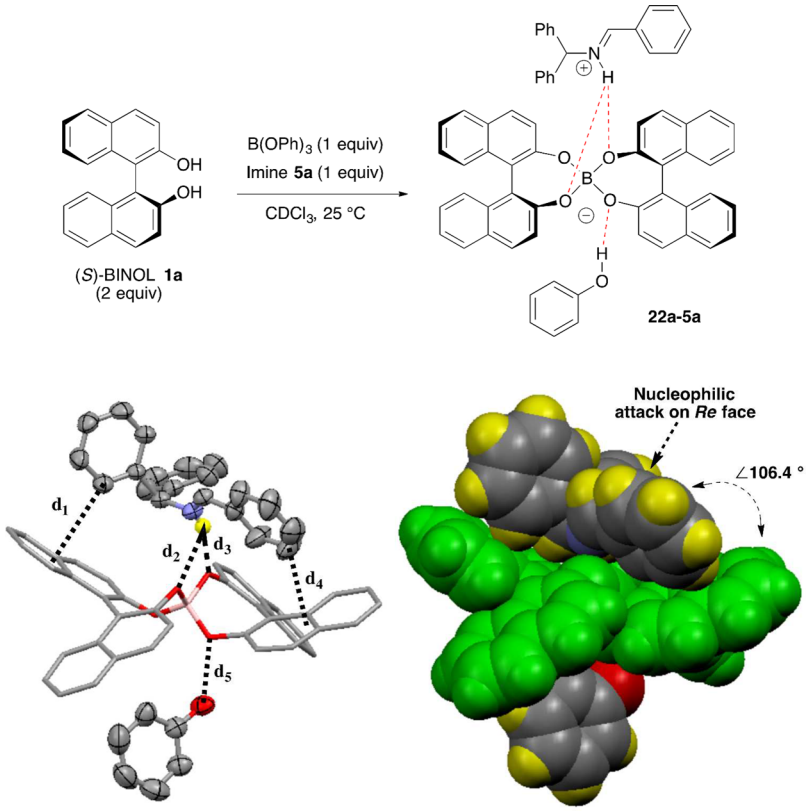

Figure 5. Crystal structure of complex **22a−5a** visualized by the Mercury Program. Calculated hydrogens and solvent molecules were omitted for clarity. Parameters for major secondary interactions: d_1 = 3.40 Å, d_2 = 2.58 Å, d_3 = 2.05 Å, d_4 = 3.60 Å, d_5 = 2.71 Å. The *spiro*-borate anion is shown in green.

iminium bond) forms an angle of 106.4° with a naphthalene ring of one of the BINOLs. The nature of the docking of imine **5a** in the *spiro*-borate catalyst derived from (*S*)-BINOL reveals that the *Re*-face of the imine is exposed to nucleophilic attack. The correlation of this observation with the actual stereoselectivity observed with *spiro*-borate catalysts of BINOL will be discussed below.

In an attempt to obtain an X-ray structure of the iminium catalyst complex **22a−5a** free of phenol, solutions of this *spiro*-borate were generated from the reaction of a 2:1 mixture of BINOL and BH_3·THF complex with imine **5a**, but all attempts to grow crystals of this complex were unsuccessful. We had previously found for the VAPOL boroxinate complex **12** (Scheme 1) that crystals of **12** were much easier to come by for the MEDAM imine **5b** than for the benzhydryl imine **5a** (Table 1).[14d] This also proved to be true in the present case as crystals of the catalyst−substrate complex **22a−5b** could be grown from a complex generated from BINOL **1a**, BH_3·THF, and imine **5b** (2:1:1). The binding of the iminium substrate to the *spiro*-borate catalyst is essentially unchanged from that of complex **22a−5a** in spite of the fact that it does not have an H-bonded phenol. The bifurcated H-bond (Figure 6, d_2 and d_3) could also be located so that it links the two ions in the ion pair. The two CH−π interactions between the edges of the phenyl rings of the iminium and the faces of the naphthalene rings of the catalyst are also present (Figure 6, d_1 and d_4). The angle between the benzylidene unit of the iminium and the naphthalene of one of the BINOLs is a little closer to perpendicular in the present case (97.3°). An additional interaction is present in the structure of **22a−5b** that is not in **22a−5a**, a CH−π interaction between the one of the methyl groups of the imine **5b** and one of the naphthalene rings of the catalyst (Figure 6, d_5). This same type of interaction exists in the substrate−catalyst complex **12** (Scheme 1) derived from the same imine and the VAPOL ligand which gives a boroxinate catalyst. However, the binding of the rest of the imine in complex **12** is very different than that in the complex **22a−5b**. As for complex **22a−5a**, the binding of the iminium in complex **22a−5b** indicates that the *Re*-face of the iminium is the one that is most open to nucleophilic attack and how this correlates with stereoselectivity in the aziridination reactions will be considered below.

Borate Esters from a 1:3 Ratio of BINOL and $B(OPh)_3$. Our venture into the arena of borate complexes with BINOL began with trying to understand why BINOL does not produce an effective catalyst for the aziridination reaction when catalyst preparation was performed with the same protocol used in the aziridination reaction with VANOL and VAPOL ligands shown in Scheme 1. Precatalyst formation was performed in the same way by heating (*S*)-BINOL with 3 equiv of commercial $B(OPh)_3$; however, unlike VAPOL and VANOL which give mixtures of *meso*- and *pyro*-borates, the reaction with BINOL gives clean conversion to the *pyro*-borate **19a** shown in Scheme 6. The ^{1}H NMR spectra of this reaction mixture are shown in Figure 2 (entry 4) and reveal that BINOL reacts to give essentially a single species with at most trace amounts of Kaufmann's propeller **17** or any other species containing a BINOL ligand. The main contaminants in this mixture are unreacted $B(OPh)_3$ and a trace amount of triphenoxyboroxine **20** (Scheme 3), as evidenced by the ^{1}H NMR spectrum with the aid of independently prepared and purified samples of each (see the Supporting Information).

DOI: 10.1021/jacs.7b02317
J. Am. Chem. Soc. 2017, 139, 10267−10285

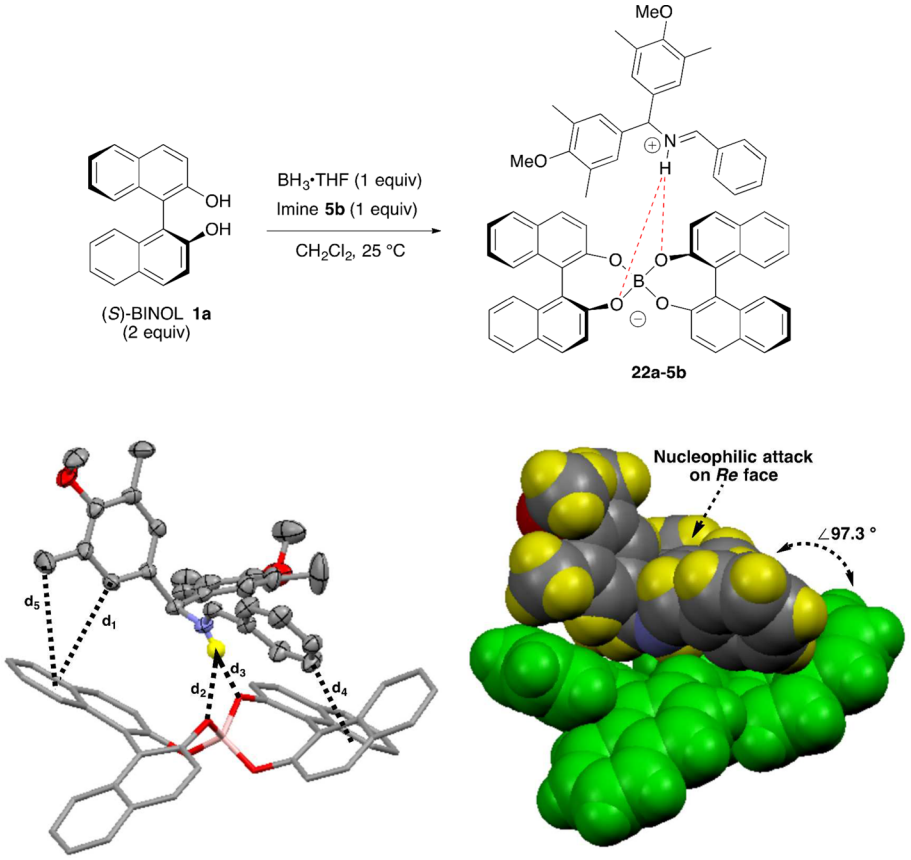

Figure 6. Crystal structure of complex **22a−5b** visualized by the Mercury Program. Calculated hydrogens and solvent molecules were omitted for clarity. Parameters for major secondary interactions: d_1 = 3.81 Å, d_2 = 2.37 Å, d_3 = 2.01 Å, d_4 = 3.38 Å, d_5 = 4.28 Å. The *spiro*-borate anion is shown in green.

Scheme 6

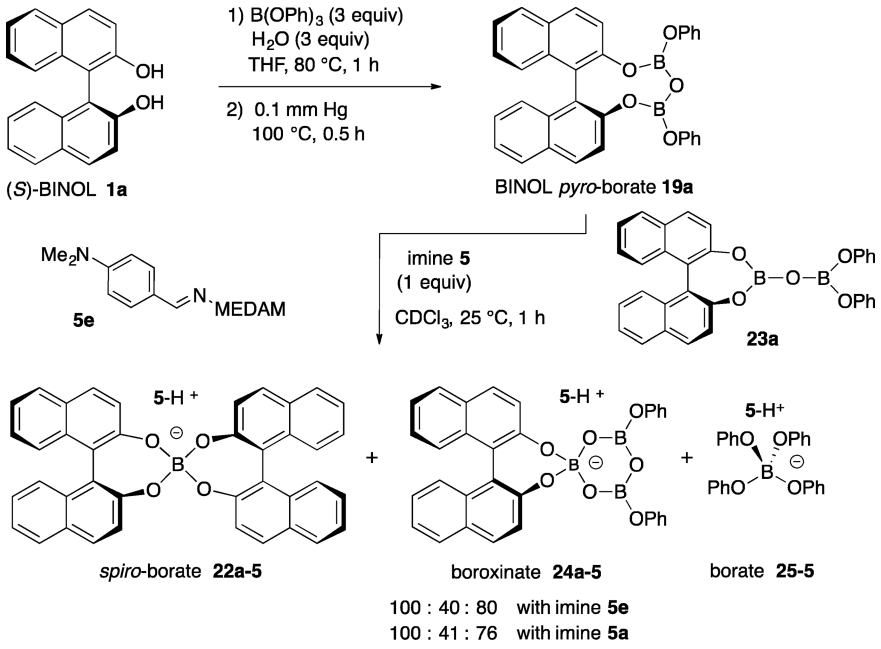

The *pyro*-borate **19a** can also be generated by heating BINOL with 2 equiv of $BH_3{\cdot}SMe_2$, 3 equiv of phenol, and 1 equiv of H_2O (Figure 2, entry 3). The H_2O is necessary to make the B−O−B linkage. Even heating BINOL with 3 equiv of $BH_3{\cdot}SMe_2$, 2 equiv of phenol, and 3 equiv of H_2O afforded *pyro*-borate **19a** as the major compound (Figure 2, entry 5). The *pyro*-borate **19a** was characterized as the mixture obtained by the method shown in Scheme 6 which produced **19a** as essentially the only BINOL containing species in the mixture (Figure 2, entry 4). While the NMR and mass spectral data

DOI: 10.1021/jacs.7b02317
J. Am. Chem. Soc. 2017, 139, 10267−10285

Scheme 7

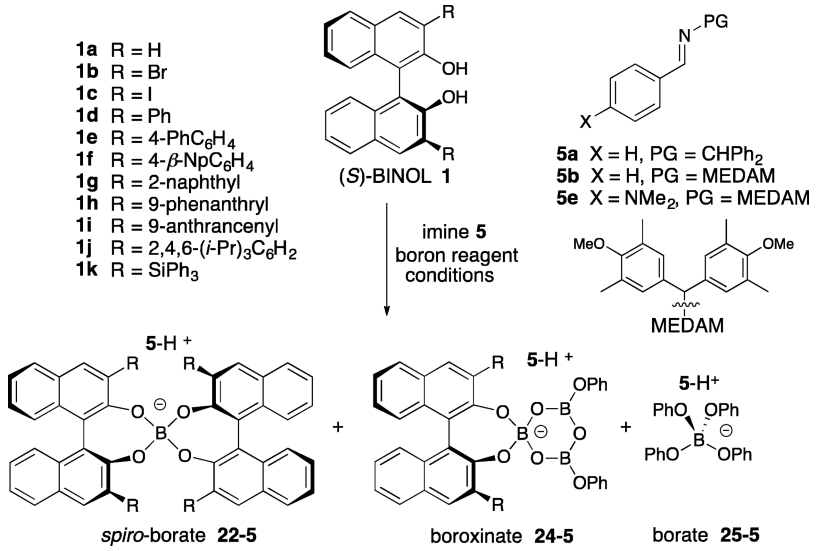

were consistent with the structure of the cyclic *pyro*-borate **19a**, an alternative linear *pyro*-borate structure would be **23a**. The assignment of all of the protons of the cyclic *pyro*-borate **19a** was made on the basis of ^{1}H NMR experiments that were employed in the assignment of the structure of the *pyro*-borate **11** of VAPOL[14f] that involved preparing the *pyro*-borate from per-deuterated triphenylborate, and these experiments are detailed in the Supporting Information. In addition, the cyclic *pyro*-borate **19a** was found to be 5.22 kcal/mol more stable than the linear *pyro*-borate **23a**, as determined at the B3LYP/6-311+G(d,p)//B3LYP/6-31G(d) level of theory and the details can be found in the Supporting Information. The energy minimized structure for the cyclic *pyro*-borate **19a** has one of the ortho-hydrogens of one of the phenoxy groups within a distance (C−C, 4.8 Å) compatible with a CH−π interaction with a naphthalene ring (see the Supporting Information). In the energy minimized structure for the linear *pyro*-borate **23a**, the closest such interaction is 5.4 Å. Since the doublet at δ = 6.17 ppm (Figure 2) has been assigned as the ortho-hydrogens on the phenoxy groups, this chemical shift is most consistent with the cyclic *pyro*-borate **19a**. The overall finding is that BINOL has a much greater propensity for the *pyro*-borate over the *meso*-borate than either VANOL or VAPOL (Scheme 1 vs Scheme 6).

While the reaction of VAPOL with 3 equiv of $B(OPh)_3$ gives a mixture of *meso*-and *pyro*-borates **10** and **11**, subsequent reaction with an imine gives the active catalyst as a single species, the ion pair **12**, which contains a chiral boroxinate anion with a boroxine core (Scheme 1). The opposite situation pertains to BINOL. The reaction of 3 equiv of $B(OPh)_3$ with BINOL **1a** gives a single species (*pyro*-borate **19a**), but the subsequent reaction with an imine **5e** gives a 5:2 mixture of the *spiro*-borate **22a−5e** and the boroxinate **24a−5e**, respectively, along with the tetra-phenoxyborate **25a−5e** (Scheme 6). A very similar ratio was noted with the imine **5a** (Scheme 6 and Table 1). The presence of each of these species is most easily determined from the ^{11}B NMR spectrum. The distribution of these three species as a function of the nature of the BINOL ligand, the type of imine, and the stoichiometry of $B(OPh)_3$ has been investigated, and the results are summarized in Figure 7.

First, it is to be noted that, when the stoichiometry of the ligand, $B(OPh)_3$, and imine is 2:1:1, a clean formation of the *spiro*-borate complex **22a** is observed and this is true with imines **5a** and **5e**, as shown by the presence of a sharp peak around $\delta \sim 9$ ppm (Figure 7a, entries 3−4) in the ^{11}B NMR spectrum. The *spiro*-borate **22a** can also be generated as a phenol free solution from the reaction of BH_3·THF with BINOL and imine **5b** (Figure 7a, entry 5). Interestingly, the aziridine **7a** (Table 1) is not a strong enough base to assemble the *spiro*-borate anion **22a** (Figure 7a, entry 6). When the ratio of BINOL to $B(OPh)_3$ is 1:4, one no longer sees a clean formation of the *spiro*-borate **22a** (Figure 7a, entries 4 vs 8). Instead, a 5:2:4 mixture of the *spiro*-borate **22a**, the boroxinate **24a**, and the nonchiral borate **25a** is observed. The major BINOL containing species is still the *spiro*-borate **22a**, but the appearance of a peak at $\delta \sim 6$ ppm indicates that the boroxinate **24a** is also formed under these conditions. A number of different boroxinate complexes of VANOL and VAPOL of the type **12** (Scheme 1) all have absorptions in the range 5−6 ppm.[14d] We assume that the anionic BINOL borates species **22a** and **24a** are in equilibrium, and since the *spiro*-borate **22a** is still the major species in the presence of 4 equiv of $B(OPh)_3$, one can deduce that the equilibrium favors the *spiro*-borate **22a**. In support of this assumption, Bull, James, and co-workers have observed dynamic ligand exchange of BINOL between chiral and nonchiral boron−aryloxy complexes in a heteroatom Diels−Alder reaction.[37] As expected, the neutral *pyro*-borate **19a** is the major species in the presence of excess $B(OPh)_3$ prior to the addition of imine **5e**. The borate species **25** with the absorption at $\delta \sim 2$ ppm in the ^{11}B NMR spectrum can also be formed from just $B(OPh)_3$ and imine **5e** (entry 1), and thus, this species was determined not to contain a molecule of BINOL. The assignment of the peak at $\delta \sim 2$ ppm as the tetraphenoxyborate **25** is based on literature values for related tetraaryloxy borate salts.[52] For the ^{1}H NMR spectra corresponding to the entries in Figure 7a, see the Supporting Information.

A significantly different outcome is observed when 3,3′-disubstituted BINOL derivatives are treated with $B(OPh)_3$ (4 equiv) and then with an imine (Scheme 7). For the 3,3′-diphenyl BINOL **1d**, only the boroxinate **24d−5a** is formed with imine **5a** (along with tetraaryloxyborate **25−5a**) and there is at most a trace of the *spiro*-borate **22d−5a** (Figure 7a, entry 10). This is interpreted to be the consequence of steric

DOI: 10.1021/jacs.7b02317
J. Am. Chem. Soc. 2017, 139, 10267−10285

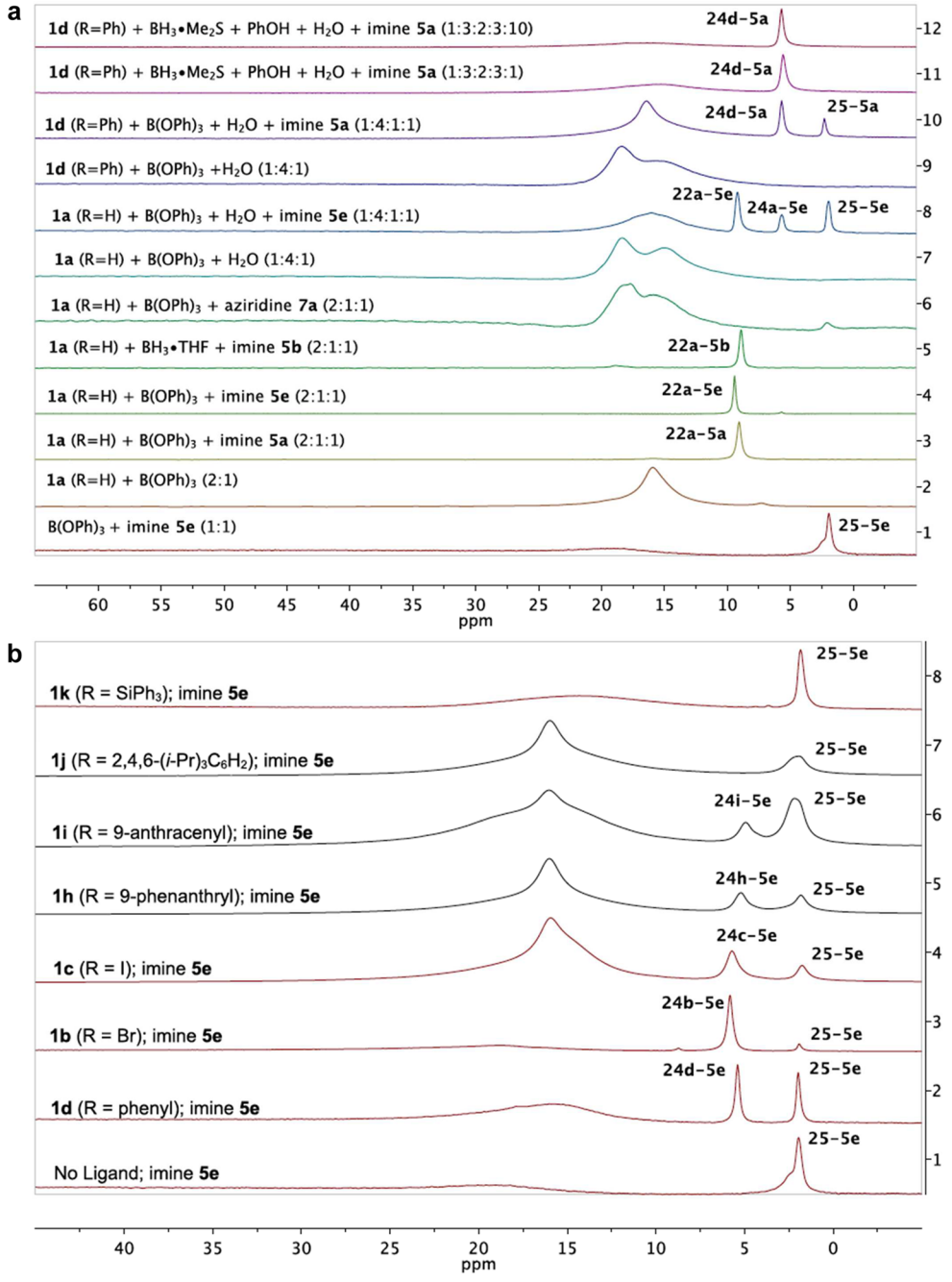

Figure 7. (a) ^{11}B NMR spectra of the boron complex derived from BINOL **1a** and **1d** in $CDCl_3$. $B(OPh)_3$ was used as purchased unless otherwise specified. All NMR spectra were acquired within 10 min after the sample was prepared. (1) Mixture of $B(OPh)_3$ and imine **5e** (1:1). (2) Mixture of (*S*)-BINOL **1a** and purified $B(OPh)_3$ (2:1). (3) Mixture of (*S*)-BINOL **1a**, purified $B(OPh)_3$, and imine **5a** (2:1:1). (4) Mixture of (*S*)-BINOL, purified $B(OPh)_3$, and imine **5e** (2:1:1). (5) Mixture of (*S*)-BINOL **1a**, BH_3·THF, and imine **5b** (2:1:1). (6) Mixture of (*S*)-BINOL **1a**, purified $B(OPh)_3$, and aziridine (*R*,*R*)-**7a** (2:1:1); a similar spectrum was observed with (*S*,*S*)-**7a**. (7) Precatalyst made by heating a 1:4:1 mixture of (*S*)-BINOL **1a**, $B(OPh)_3$, and H_2O in toluene at 80 °C for 1 h and then removal of volatiles. (8) Mixture of imine **5e** and precatalyst (1:1) made in entry 7. (9) Precatalyst made by heating a 1:4:1 mixture of substituted (*S*)-BINOL **1d**, $B(OPh)_3$, and H_2O in toluene at 80 °C for 1 h and then removal of volatiles. (10) Mixture of imine **5a** and precatalyst (1:1) made in entry 9. (11) A 1:1 mixture of imine **5a** and precatalyst prepared by reaction of (*S*)-BINOL **1d**, BH_3·SMe_2, PhOH, and H_2O (1:3:2:3) in toluene at 100 °C for 1 h and then removal of the volatiles. (12) A 10:1 mixture of imine **5a** and precatalyst prepared by reaction of (*S*)-BINOL **1d**, BH_3·SMe_2, PhOH, and H_2O (1:3:2:3) in toluene at 100 °C for 1 h and then removal of the volatiles. (b) ^{11}B NMR spectra of the boron complex derived from BINOL analogues in $CDCl_3$. $B(OPh)_3$ was used as purchased unless otherwise specified. (1) Mixture of $B(OPh)_3$ and imine **5e** (1:1). (2) Mixture of imine **5e** and precatalyst (1:1) made by heating a 1:4:1 mixture of (*S*)-BINOL **1d**, $B(OPh)_3$, and H_2O in toluene at 80 °C for 1 h and then removal of volatiles. (3) Mixture of imine **5e** and preformed catalyst (1:1) made from substituted (*S*)-BINOL **1b**, $B(OPh)_3$, and H_2O (1:4:1). (4) Mixture of imine **5e** and preformed catalyst (1:1) made from substituted (*S*)-BINOL **1c**, $B(OPh)_3$, and H_2O (1:4:1). (5) Mixture of imine **5e** and preformed catalyst (1:1) made from substituted (*S*)-BINOL **1h**, $B(OPh)_3$, and H_2O (1:4:1). (6) Mixture of imine **5e** and preformed catalyst (1:1) made from substituted (*S*)-BINOL **1i**, $B(OPh)_3$, and H_2O (1:4:1). (7) Mixture of imine **5e** and preformed catalyst (1:1) made from substituted (*S*)-BINOL **1j**, $B(OPh)_3$, and H_2O (1:4:1). (8) Mixture of imine **5e** and preformed catalyst (1:1) made from substituted (*S*)-BINOL **1k**, $B(OPh)_3$, and H_2O (1:4:1).

DOI: 10.1021/jacs.7b02317
J. Am. Chem. Soc. 2017, 139, 10267–10285

Table 2. Catalysts Derived from BINOL 1a and 1d in the Catalytic Asymmetric Aziridination Reaction[a]

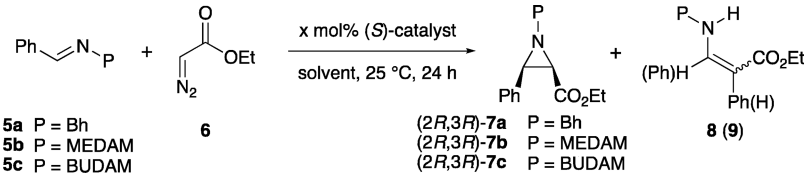

5a P = Bh
5b P = MEDAM
5c P = BUDAM

6

(2*R*,3*R*)-**7a** P = Bh
(2*R*,3*R*)-**7b** P = MEDAM
(2*R*,3*R*)-**7c** P = BUDAM

8 (**9**)

entry	P	ligand	mol% catalyst	method[b]	$B(OPh)_3$ /ligand ratio	solvent	% yield *cis*-**7**[c]	cis/trans **7**[d]	% ee **7**[e]	% yield **8** : **9**[d]
1	Bh	none	0	A'	—	toluene	78	>50:1	—	8/2
2	Bh	(S)-VAPOL **4**	10	A	3 : 1	toluene	80[f]	>50:1	91	5/6
3	Bn	(S)-VAPOL **4**	10	A	1 : 2	toluene	75	7 : 1	78	nd
4	Bh	(S)-VAPOL **4**	5	B	4 : 1	toluene	82[g]	≥50:1	94	<1
5	Bh	(S)-VAPOL **4**	5	B	4 : 1	CH_2Cl_2	67[g]	≥33:1	91	2
6	MEDAM	(S)-VAPOL **4**	5	B	4 : 1	toluene	98[h]	≥33:1	99	2
7	BUDAM	(S)-VAPOL **4**	2	C	3 : 1	toluene	98[i]	≥50:1	99	≤2
8	Bh	(*S*)-BINOL **1a**	10	A	3 : 1	toluene	63	18:1	13	3/4
9	Bh	(*S*)-BINOL **1a**	10	C	3 : 1	toluene	66	>50:1	13	10/7
10	Bh	(*S*)-BINOL **1a**	10	D	3 : 1	CH_2Cl_2	58[j]	18:1	24	13/9
11	MEDAM	(*S*)-BINOL **1a**	5	B	4 : 1	toluene	72[h]	17:1	38	24
12	BUDAM	(*S*)-BINOL **1a**	10	D	3 : 1	CH_2Cl_2	71[i]	nd	67	nd
13	Bh	(*S*)-BINOL **1a**	10	E	1 : 2	CH_2Cl_2	44[l]	8:1	–26[k]	24/23
14	Bh	(*R*)-BINOL **1a**	100	E	1 : 2	CH_2Cl_2	8	50:1	76	5/5
15	MEDAM	(*S*)-BINOL **1a**	10	F	1 : 2	CH_2Cl_2	36	2:1	–63[k]	18/8
16	Bh	(*S*)-**1d**	10	A	3 : 1	toluene	84	50:1	75	7/8
17	Bh	(*S*)-**1d**	10	B	4 : 1	toluene	90	>50:1	76	4/6
18	Bh	(*S*)-**1d**	10	C	3 : 1	toluene	84[m]	40:1	70	4/5
19	Bh	(*S*)-**1d**	10	C	3 : 1	CH_2Cl_2	80[n]	19 : 1	53	nd
20	Bh	(*S*)-**1d**	10	G	3 : 1	toluene	89	50:1	76	4/7
21	MEDAM	(*S*)-**1d**	10	B	4 : 1	toluene	89	>50:1	79	2/6
22	MEDAM	(*S*)-**1d**	10	G	3 : 1	toluene	85	25:1	78	5/9
23	BUDAM	(*S*)-**1d**	10	B	4 : 1	toluene	88	>50:1	76	4/8
24	BUDAM	(*S*)-**1d**	10	G	3 : 1	toluene	90	>50:1	90	1/7

[a]Unless otherwise specified, all reactions were run with 1.0 mmol of imine at 0.5 M and 1.2 equiv of **6** at 25 °C for 24 h. [b]A′: reaction performed with 0.4 equiv of $B(OPh)_3$ and 1.0 equiv of **5a** with 1.2 equiv of **6**. A: catalyst was directly generated by mixing of **1** equiv of (*S*)-ligand, 3 equiv of $B(OPh)_3$, and 10 equiv of imine **5a** in toluene at 25 °C for 5 min. B: precatalyst prepared by reaction of (*S*)-ligand with 4 equiv of $B(OPh)_3$ and 1 equiv of H_2O in toluene at 80 °C for 1 h and then removal of volatiles. C: precatalyst prepared by reaction of (*S*)-ligand with 3 equiv of $B(OPh)_3$ in toluene at 80 °C for 1 h and then removal of volatiles. D: precatalyst prepared by reaction of (*S*)-ligand with 3 equiv of $B(OPh)_3$ in CH_2CI_2 at 55 °C for 1 h and then removal of volatiles. E: reaction performed by adding 12 equiv of **6** to a CH_2CI_2 solution of a (2:1:10) mixture of **1a**, $B(OPh)_3$, and imine **5a**. F: Catalyst prepared by stirring a solution of 2 equiv of BINOL with 1 equiv of BH_3·THF and 1 equiv of amine **5b** for 30 min and then removal of volatiles. After dissolution, 9 equiv of **5b** and 12 equiv of **6** were added. G: precatalyst prepared by reaction of the ligand, BH_3·Me_2S, PhOH, and H_2O (1:3:2:3) in toluene at 100 °C for 1 h and then removal of the volatiles. [c]Isolated yield after silica gel chromatography. [d]Determined from the ^1H NMR spectrum of the crude reaction mixtures. [e]Determined by HPLC on purified *cis*-**7**. [f]Reference 14d. [g]Reference 14a. [h]Reference 14c. [i]Reference 14b. [j]Average of three runs. [k]Enantiomer of **7** was obtained. [l]Average of four runs. [m]Average of two runs. [n]Average of three runs.

interactions between the Ph groups on one BINOL with those on another in the possible *spiro*-borate species **22d**–**5a**. Also to be noted is that the spectrum does not change whether 1 or 10 equiv of the imine **5a** is added (Figure 7a, entries 11 and 12). Among other BINOL derivatives, boroxinate species of the type **24** were observed with ligands **1b** (R = Br) and **1c** (R = I) (Figure 7b, entries 3 and 4). As was the case for BINOL **1d** (Figure 7b, entry 2), no *spiro*-borate **22b**/**22c** was formed with BINOL **1b** or **1c**, as noted by the absence of absorptions at ∼9–10 ppm in entries 3 and 4 of Figure 7b. Only small amounts of boroxinates **24h**/**24i** were obtained in the cases of BINOL derivatives **1h** (R = 9-phenanthryl) and **1i** (R = 9-anthracenyl) (Figure 7b, entries 5 and 6). The introduction of the very large 2,4,6-(*i*-Pr)$_3$C$_6$H$_2$ groups in the 3- and 3′-positions of BINOL (**1j**) causes the boron to forego incorporation into either the *spiro*-borate **22j** or the boroxinate **24j** (Figure 7b, entry 7). The only borate species observed in this case is the tetra-phenoxyborate **25** which exists as a salt with the protonated form of imine **5e**. A similar observation was made in the case of the BINOL derivative **1k** with large triphenylsilyl groups at the 3- and 3′-positions (Figure 7b, entry 8).

Comparison of the BINOL *spiro*-Borate 22 and the BINOL Boroxinate 24 as Catalysts in the Aziridination Reaction. We have not observed a *spiro*-borate species of the type **22** with either the VAPOL or VANOL ligand, although this will be the subject of additional study. The fact that BINOL can be induced to cleanly generate the *spiro*-borate **22** presented the opportunity to investigate the ability of this chiral borate to induce asymmetric induction in the

DOI: 10.1021/jacs.7b02317
J. Am. Chem. Soc. 2017, 139, 10267–10285

aziridination of imines with ethyl diazoacetate. The data in Table 2 include results with catalysts generated with both a 1:2 and a 3−4:1 ratio of $B(OPh)_3$ to BINOL. For comparison, results of catalysts prepared from a 1:2 and a 3−4:1 ratio of $B(OPh)_3$ to VAPOL are also included in the table (entries 2 and 3). Our previous studies indicate that VAPOL does not form a *spiro*-borate for steric reasons, and thus, the result in entry 3 is thought to most likely involve a boroxinate catalyst. A control experiment was performed where only $B(OPh)_3$ was used as the catalyst (no ligand) and a 78% yield of the aziridine **7a** was isolated (entry 1). Since it was shown that the reaction of $B(OPh)_3$ and an imine can generate the tetraphenoxyborate **25** (Figure 7a, entry 1), this control experiment provides evidence that this species catalyzes the background reaction. However, as will be discussed below, we have evidence that the background reaction is not the source of the lower inductions for the BINOL catalyst. As has been determined to be the case for VAPOL,[14b] BINOL catalysts give higher asymmetric inductions in the series, BUDAM imines > MEDAM imines > benzhydryl imines, under boroxinate forming conditions with a 3:1 ratio of $B(OPh)_3$/BINOL (Table 2, entries 10−12). As was shown by the ^{11}B NMR spectra in entries 3−5 in Figure 7a, the use of a 1:2 ratio of $B(OPh)_3$ to BINOL gives the clean formation of the *spiro*-borate **22**, and as can be seen from entry 13 in Table 2, this species does catalyze the aziridination and gives the aziridine **7a** in 26% ee. The asymmetric induction can be increased from 26% ee to 76% ee with 100 mol % catalyst, but for reasons we do not understand, the yield falls to 8% (entry 14). The % ee can also be increased by using the MEDAM imine **5b**, giving **7b** in 63% ee (entry 15). When the ratio of $B(OPh)_3$ to BINOL is 3:1, a mixture of *spiro*-borate **22** and boroxinate **24** is produced, as indicated by the ^{11}B NMR spectra, and as indicated in Scheme 6, the ratio of **22**:**24** is 100:40 with imines **5e** and 100:41 with imine **5a**. For imine **5a**, this catalyst mixture results in the formation of the aziridine **7a** in 24% ee, and this rises to 67% ee with the BUDAM imine **5c** (entries 10 and 12). For the boroxinate catalysts of VANOL and VAPOL, it has been found that the asymmetric inductions of a range of substrates are slightly higher for toluene as solvent than methylene chloride.[14a] This solvent effect was found also to be true for the boroxinate catalyst generated from the BINOL ligand **1d** (entries 18 vs 19). The ^{11}B NMR spectra reveal that ligand **1d** forms the boroxinate species to the exclusion of the *spiro*-borate (Figure 7a, entries 10−12). However, the catalysts generated from a 1:2 ratio of $B(OPh)_3$ to BINOL could not be studied in both solvents. This catalyst mixture was not soluble in toluene but was completely soluble in methylene chloride (entry 13). When the reaction in entry 13 is run in toluene, there is a solid present in the reaction mixture during the entire course of the reaction and the results are variable and not deemed reliable (see the Supporting Information). On the other hand, the catalyst generated from a 3:1 ratio of $B(OPh)_3$ and BINOL is soluble in toluene (entries 8 and 9).

The most interesting observation to be made from the data in Table 2 is that the BINOL catalyst prepared with a 1:2 ratio of $B(OPh)_3$ to BINOL gives the opposite configuration of aziridine **7a** than the catalyst generated from a 4:1 ratio (entries 10 vs 13). Since the former gives a catalyst consisting of just the *spiro*-borate **22a** (Figure 7a, entry 3) and the latter gives a catalyst consisting of a mixture of the *spiro*-borate **22a** and the boroxinate **24a** (Figure 7a, entry 3), this suggests that, as catalysts, the *spiro*-borate **22a** and the boroxinate **24a** give opposite asymmetric inductions in the aziridination reaction. The ^{11}B NMR studies summarized in Figure 7 reveal that the 3,3′-diphenyl BINOL ligand **1d** produces a catalyst that contains only the boroxinate **24** and none of the *spiro*-borate **22** (Figure 7a, entries 10−12) Thus, this presents an opportunity to determine how the BINOL boroxinate catalyst **24** with the boroxinate core will function in the aziridination catalyst unencumbered by the presence of the competing *spiro*-borate catalyst **22** and, furthermore, to determine how it compares to the boroxinate VAPOL catalyst **12**. As expected, the diphenyl BINOL derivative **1d** gave much higher asymmetric induction than the unsubstituted BINOL, giving 70% ee under conditions where BINOL gives only 13% ee (Table 2, entry 16 vs entry 8). This is still as significantly lower selectivity than that observed for the boroxinate VAPOL catalyst **12** under the same conditions (91% ee, Table 2, entry 2). These results reveal that, while the (*R*)-enantiomer of the pure BINOL boroxinate catalyst **24d** gives the (2*S*,3*S*)-aziridine **7a**, the same enantiomer of this aziridine is obtained from the (*S*)-enantiomer of the pure *spiro*-borate BINOL catalyst **22a**. Interestingly, an asymmetric induction up to 90% ee was obtained with the BUDAM phenyl imine **5c** when the boron source was switched from $B(OPh)_3$ to $BH_3{\cdot}SMe_2$ (entry 23 vs entry 24). However, no significant changes were observed for the imines **5a** and **5b** (entries 17 vs 21 and entries 20 vs 22). Additionally, comparable results were obtained when the catalyst was formed from BINOL **1d** by the direct method involving simply mixing **1d** with $B(OPh)_3$ and imine **5a** as when the catalyst was prepared by the indirect method involving the initial generation of a precatalyst, as indicated in Scheme 1 (75% ee, entry 16 vs 76% ee, entry 17). It should be noted that Chen and co-workers reported a huge drop in enantioinduction (34% ee) using BINOL derivative **1d** and an imine derived from 4-CH_3SO_2−C_6H_4CHO for the catalytic asymmetric aziridination reaction.[14e]

A question arises in comparing the asymmetric induction observed for the VAPOL boroxinate catalyst (94% ee, Table 2, entry 4) and the BINOL boroxinate catalyst (76% ee, Table 2, entry 17). Is this difference the result of an inherent difference in the boroxinate complex **12** with VAPOL and the boroxinate complex **24d** for the BINOL ligand **1d**? Alternatively, could the difference be due to a greater background reaction by the nonchiral borate species **25** for the BINOL boroxinate than for the VAPOL boroxinate? We have obtained evidence that this is not the case. Depending on the stoichiometry, varying amounts of the nonchiral borate species **25** are formed. For example, the BINOL boroxinate **24d** generated from the reaction of the BINOL ligand **1d** with 4 equiv of a boron precursor is formed with significant amounts of the nonchiral borate **25** (38% of **24d**) (Figure 7a, entry 10), whereas, with only 3 equiv of boron, the boroxinate **24d** is formed with no discernible amount of the nonchiral borate **25** (Figure 7a, entry 11). Despite this, the formation of the BINOL boroxinate **24d** under these two conditions gives the same asymmetric induction (Table 2, entries 17 and 20).

In order to examine the electronic and steric effects of other substituted BINOL ligands, a series of catalysts were generated from several different 3,3′-disubstituted BINOLs with 3−4 equiv of $B(OPh)_3$ (or $BH_3{\cdot}SMe_2$ and PhOH) and the results from the screening of these catalysts in the aziridination of imines **5a** and **5f** with ethyl diazoacetate are presented in Table 3. Since the ^{11}B NMR spectra revealed that the dibromo and diiodo BINOL derivatives **1b** and **1c** gave relatively clean

DOI: 10.1021/jacs.7b02317
J. Am. Chem. Soc. 2017, 139, 10267−10285

Table 3. 3,3′-Disubstituted BINOL Catalysts for Asymmetric Aziridination[a]

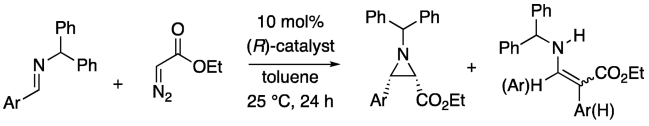

5a (Ar = C_6H_5) **6** (2*S*,3*S*)-**7a** (Ar = C_6H_5) **8 (9)**
5f (Ar = 4-BrC_6H_4) (2*S*,3*S*)-**7f** (Ar = 4-BrC_6H_4)

entry	imine	BINOL	R in BINOL	method [b]	% yield **7**	% ee [d] **7**	% yield **8 (9)** [e]
1	**5a**	**1a**	H	C	66	13	10/7
2	**5a**	**1b**	Br	B	89	55	4/3
3	**5a**	**1c**	I	B	80	51	6/6
4	**5a**	**1d**		B	90	76	4/6
5		**1d**		C	88	75	4/5
6 [f]		**1d**		C	91	76	1/5
7		**1d**		G	85	78	3/9
8 [g]	**5f**	**1e**		D	68	69	—
9 [g]	**5f**	**1f**		D	76	78	—
10 [g]	**5a**	**1f**		D	55	54	—
11 [g]	**5f**	**1g**		D	63	58	—
12	**5a**	**1h**		B	50 [h]	13	10/11
13	**5a**	**1i**		B	75 [i]	3	13/10
14	**5a**	**1j**		B	78	–2	5/9
15	**5a**	**1j**		H	55	–0.4	8/10
16	**5a**	**1k**	$SiPh_3$	B	80	1	2/2

[a]Unless otherwise specified, all reactions were run with 1.0 mmol of imine at 0.5 M in toluene and 1.2 equiv of **6** at 25 °C for 24 h. The cis:trans selectivity was >50:1 unless otherwise specified. [b]The reactions were run with 10 mol % of a catalyst prepared from the (*R*)-enantiomer of the ligand. Methods B–G are given in Table 2. Method H: A solution of the ligand, 4 equiv of $B(OPh)_3$, and 10 equiv of imine was heated in toluene at 80 °C for 0.5 h and then cooled to 25 °C, and 12 equiv of **6** was added to start the reaction. [c]Isolated yield after silica gel chromatography. [d]Determined by HPLC on purified *cis*-**7**. [e]Determined from the ^{1}H NMR spectrum of the crude reaction mixture. [f]Reaction at 0 °C. [g]Reference 28. [h]cis:trans = 15:1. [i]cis:trans = 25:1.

catalysts that contained the boroxinate complex **24b**/**24c** but at most traces of the *spiro*-borate **22b**/**22c** (Figure 7b, entries 3 and 4), these catalysts as expected gave higher asymmetric inductions (~50% ee) than the BINOL itself (Table 3, entries 2 and 3 vs entry 1). The finding that 3,3′-disubstituted BINOL derivatives give higher asymmetric inductions in the aziridination reaction than the parent BINOL had been previously observed by Wipf and Lyon (entries 8–11).[28] Interestingly, while they tried ligands bearing meta- (entry 11) and para-substituted aryl rings (entries 8–10) at the 3,3′ positions, no ligand bearing an ortho-substituted aryl ring was examined nor was the unsubstituted phenyl analog **1d** examined. The observation that the BINOL derivative **1j** (R = 2,4,6-(*i*-Pr)$_3$C$_6$H$_2$) containing *iso*-propyl groups in the ortho-positions gives the aziridine **7a** in −2% ee (entry 14) was in fact anticipated from the ^{11}B NMR spectrum in entry 7 of Figure 7b, since it reveals the absence of both the *spiro*-borate catalyst **22j** and the boroxinate catalyst **24j**. However, the reaction does occur in 78% yield (when R = 2,4,6-(*i*-Pr)$_3$C$_6$H$_2$) which can be explained by the fact that the only borate species observed in the ^{11}B NMR spectrum was the nonchiral borate **25**. Also, as expected for the same reasons, a similar observation (1% ee, entry 16) was made for the BINOL derivative **1k** (R = $SiPh_3$). While a 58% ee (entry 11) was reported by Wipf and co-workers for aziridine **7f** with a catalyst prepared from the 2-naphthyl BINOL derivative **1g** (R = 2-naphthyl), nearly racemic aziridines **7a** were obtained when the BINOL derivatives **1h** (R = 9-phenanthryl) and **1i** (R = 9-anthracenyl) were employed (entries 12–13). This suggests that ortho-substitution in an aryl ring in the 3,3′-positions of BINOL hinders the formation of the boroxinate catalyst, thus lowering the asymmetric induction. This is supported by the ^{11}B NMR spectrum which indicates the formation of a much reduced amount of the boroxinate catalyst **24h** and **24i** (Figure 7b, entries 5 and 6). It is interesting to note that the present work reveals that BINOL ligand **1d** bearing a phenyl group in the 3- and 3′-positions is superior to the BINOL ligand **1f** with a *para*-2-naphthylphenyl group (entries 5 vs 10). Finally, in 2011, Chen and co-workers reported similar observations with BINOL derivatives **1i** and **1k** when they performed catalytic asymmetric aziridination reactions with an imine derived from 4-SO_2CH_3–C_6H_4CHO.[14e]

Computational Analysis of the Asymmetric Inductions for the *Spiro*-Borate 22 and the Boroxinate 24. We investigated the origins of opposite asymmetric induction for the reaction of **5a** and **6** catalyzed by (*R*)-BINOL–*spiro*-borate **22a** and (*R*)-BINOL–boroxinate **24a** using the B3LYP[53] method employing a 6-31G* basis set (for the entire system) as implemented in Gaussian 09.[54] The mechanism of the aziridination reaction of MEDAM imine **5b** and **6** catalyzed by VANOL-based boroxinate has been established using

Scheme 8

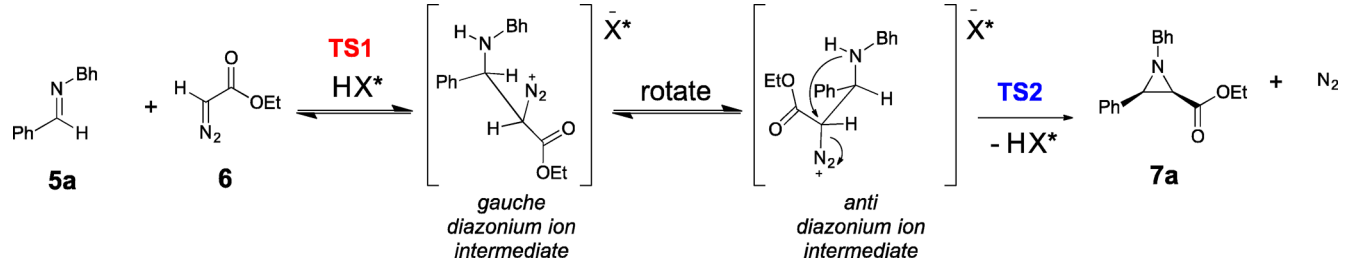

DOI: 10.1021/jacs.7b02317
J. Am. Chem. Soc. 2017, 139, 10267–10285

experimental kinetic isotope effects (KIEs) and theoretical calculations.[14g] The reaction proceeds via initial carbon−carbon bond formation (**TS1**) between **5a** and **6** to reversibly yield the diazonium ion intermediate followed by rate-determining S_N2-like attack of the imine nitrogen with concomitant displacement of N_2 (**TS2**) to furnish the final *cis*-aziridine product **7a** (Scheme 8). The origin of enantioselectivity is obtained from the relative energetics of **TS2** in the pathways leading to the major and minor enantiomers of **7a**.

Rather than assume the same mechanism for the analogous reaction catalyzed by **22a** and **24a**, we thought it appropriate to model *both* the C−C bond forming (**TS1**) and ring-closing (**TS2**) transition structures leading to *both* the major and minor enantiomers for *both* catalysts. Generation of the energy profile of the reaction coordinate is expected to provide insight into the enantiodivergence observed in reactions catalyzed by these two distinct species **22a** and **24a**. Such a comprehensive analysis of a large computational system is challenging, but our extensive experience in modeling these reactions allowed us to streamline the process. It must be noted here that the use of benzhydryl instead of MEDAM imine and BINOL instead of VAPOL significantly reduced the size of the model system compared to our previous studies. This enabled treatment of the full model system using the DFT method, which is expected to provide more reliable energetics compared to our previous studies that utilized the hybrid DFT:semiempirical ONIOM method.[14g]

The reaction pathways leading to the major and minor enantiomers of the *cis*-aziridine product **7a** catalyzed by (*R*)-BINOL−*spiro*-borate **22a** are shown in Figure 8. The highest

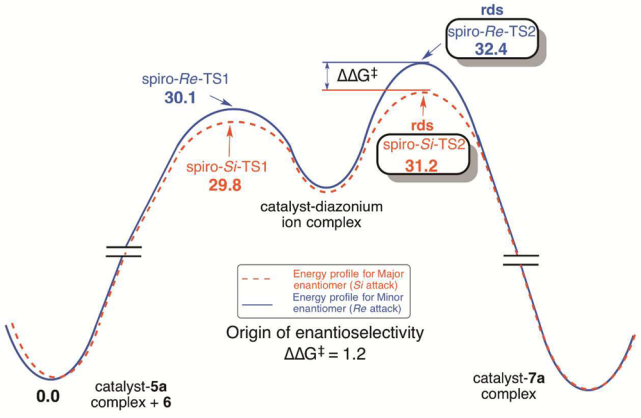

Figure 8. Reaction coordinate *spiro*-borate (**22a**) catalyzed aziridination reaction of **5a** and **6**.

energy barrier in the reaction coordinates for the major (red, *Si* attack) and minor (blue, *Re* attack) enantiomer is the S_N2-like ring-closing step. The enantioselectivity is therefore a result of the difference in energy, $\Delta\Delta G^{\ddagger}$, of the two ring-closing transition structures spiro-*Re*-TS2 and spiro-*Si*-TS2. This difference is found to be 1.2 kcal/mol, which corresponds to 82% ee at room temperature—with the preferred product corresponding to initial attack of **6** to the *Si*-face of imine **5a**. While this is an overestimation of the experimental enantioselectivity (26% ee; Table 2, entry 13), it is in qualitative agreement with experiment. All four relevant transition structures along with key distances of bond-forming and stabilizing interactions (with distances in Å) are shown in Figure 9. Rate-determining transition structures in both

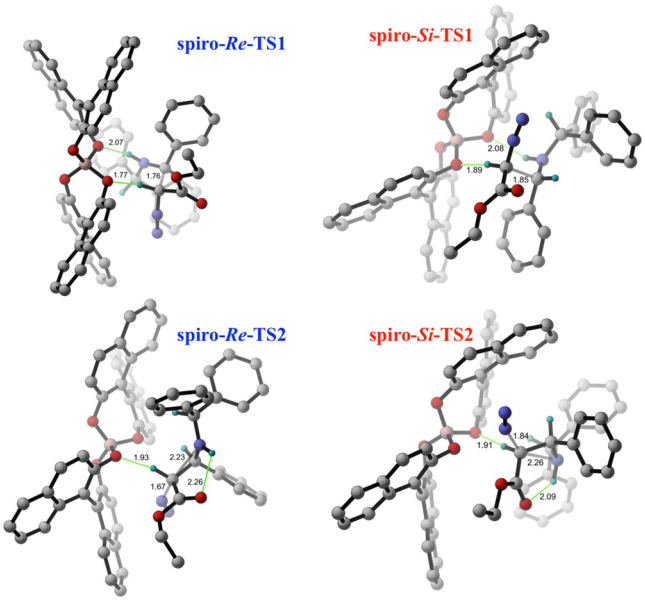

Figure 9. Relevant transition structures along the reaction coordinates leading to the major and minor enantiomers of product **7a** in the reaction of **5a** and **6** catalyzed by *spiro*-borate **22a**.

pathways (spiro-*Re*-TS2 and spiro-*Si*-TS2) benefit from similar stabilizing interactions, namely, (a) a CH···O noncovalent interaction between the *α*-CH of **6** and an anionic *spiro*-borate oxygen atom and (b) an intramolecular H-bonding interaction between the N−H and the carbonyl moiety of the diazonium ion intermediate.[55] The transition structure *spiro*-Si-TS2 is lower in energy than *spiro*-Re-TS2, since both of these interactions, (a) and (b), are enhanced in *spiro*-Si-TS2 ($r_{CH\cdots O}$ = 1.91 Å and $r_{NH\cdots O}$ = 2.09 Å) versus *spiro*-Re-TS2 ($r_{CH\cdots O}$ = 1.93 Å and $r_{NH\cdots O}$ = 2.26 Å).

The reaction pathways leading to the major and minor enantiomers of the *cis*-aziridine product **7a** catalyzed by the (*R*)-BINOL-boroxinate **24a** are shown in Figure 10. The

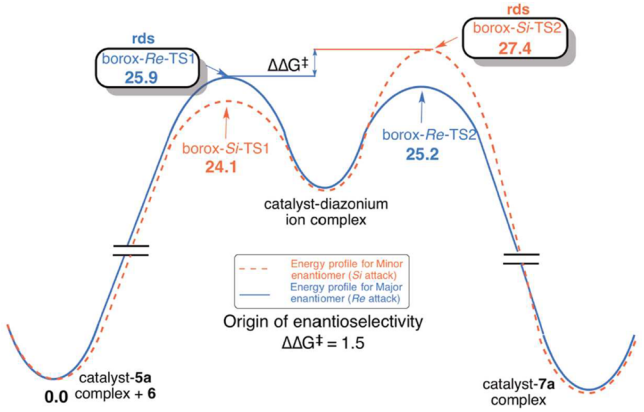

Figure 10. Reaction coordinate boroxinate (**24a**) catalyzed aziridination reaction of **5a** and **6**.

highest energy barrier along the reaction coordinate for the major enantiomer (blue, *Re* attack) is for the C−C bond-forming step (borox-*Re*-TS1). Intriguingly, the highest energy barrier for the minor enantiomer (red, *Si* attack) is the S_N2-like ring-closing step (borox-*Si*-TS2). This presents a rather unique situation where the origin of enantioselectivity in a catalytic

DOI: 10.1021/jacs.7b02317
J. Am. Chem. Soc. 2017, 139, 10267−10285

asymmetric reaction is determined by the comparison of the relative energy of different steps along the reaction coordinate of the two enantiomeric pathways. The $\Delta\Delta G^{\ddagger}$, the energy difference between these two highest energy steps, is 1.5 kcal/mol—with the preferred product corresponding to initial attack of **6** to the *Re*-face of imine **5a**. This corresponds to a prediction of 89% ee at room temperature (of the opposite enantiomer of **7a** with respect to the reaction catalyzed by **22a**) if the boroxinate catalyst could be formed exclusively. There is no experimental result corresponding to this theoretical finding, since **24a** is always formed as the minor component in the catalyst mixture, regardless of the ratio of ligand to $B(OPh)_3$ used. However, this result suggests that, if formed exclusively, **24a** would be a rather selective catalyst for this transformation. *Additionally, our computational study validates the hypothesis that the low enantioselectivity, observed when a mixture of* ***22a*** *and* ***24a*** *catalyzed the aziridination* reaction *of* ***5a*** *and* ***6****, results from the opposite absolute asymmetric induction observed with the two catalysts.* All four of the transition structures for the reaction catalyzed by **24a** along with distances for key stabilizing interactions are shown (Figure 11).

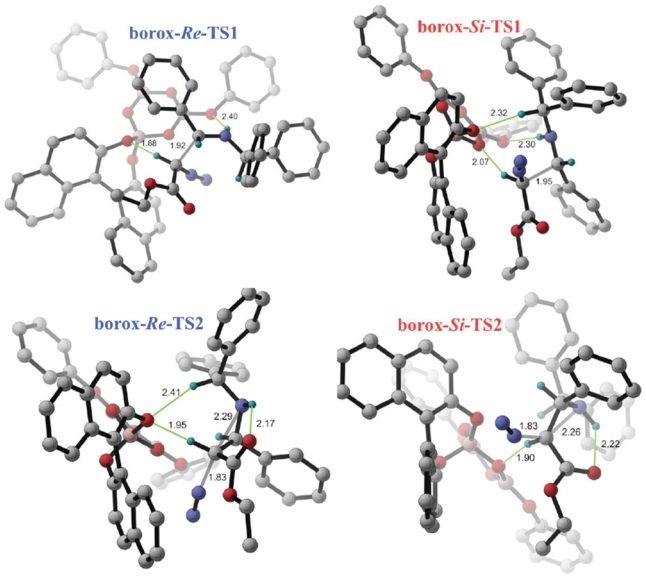

Figure 11. Relevant transition structures along the reaction coordinates leading to the major and minor enantiomers of product **7a** in the reaction of **5a** and **6** catalyzed by boroxinate **24**.

Which Is the Better Catalyst? We have shown that, when a 3:1 ratio of $B(OPh)_3$ to (*S*)-BINOL is used, (*S*)-BINOL−*spiro*-borate **22a** and (*S*)-BINOL−boroxinate **24a** are formed in the ratio of 5:2 with imine **5a** (Scheme 6 and Supporting Information). The enantiomer of the aziridine **7a** that is formed under these conditions ((*R*,*R*)-**7a**, Table 2, entry 9) does not correspond to the expected enantiomer if **22a** was the major catalyst species present in solution ((*S*,*S*)-**7a**, Table 2, entry 12). In addition to the origin of enantioselectivity with the two catalysts, our computational study provides valuable information that accounts for this seemingly counterintuitive observation. Comparison of the absolute barrier of the rate-determining steps leading to the major enantiomer of product in each of the catalytic systems (borox-*Re*-TS1 and spiro-*Si*-TS2) reveals that the borox-*Re*-TS1 has a lower barrier (25.9 kcal/mol) to catalysis than the spiro-*Si*-TS2 (31.2 kcal/mol). This energy difference corresponds to a reaction rate for **24a** that is ∼10,000 times faster than **22a**—a value that is likely inflated (due to the size of the computational system and the level of theory used) but one that provides valuable qualitative information to compare the two catalysts. This observation accounts for why even at a ratio of 5:2 of **22a**:**24a** the enantiomeric outcome of the reaction is dictated by the boroxinate catalyst **24a**.

What Is the Origin of the Reversal of Enantioselectivity? In order to answer this question, we decided to compare the absolute energy of each of the four transition structures for the two catalysts (Table 4). It is clear from Table 4 that the transition structure that benefits the most (energetically) from switching catalyst **22a** to **24a** is borox-*Re*-TS2 (7.2 kcal/mol advantage) followed by spiro-*Si*-TS1 (5.7 kcal/mol advantage). In order to understand the origin of this energetic effect, we examined these transition structures for unique features that were not present in the other six structures. We were able to find a CH···O interaction between the benzhydryl CH and one of the oxygen atoms of BINOL that was a distance of 2.41 Å in borox-*Re*-TS2 and 2.32 Å in borox-*Si*-TS1. This benzyhydryl CH is slightly acidic by virtue of being adjacent to two phenyl groups and a nitrogen atom that bears a partial positive charge at both TS1 and TS2. Such relatively weak noncovalent interactions can sometimes make significant contributions to transition state stabilization.[56,57]

Table 4. Comparison of Absolute Barriers of Each Transition State Catalyzed by the Two BINOL Based Catalysts 22a and 24a

TS Catalyst **22a**	$\Delta G^{\ddagger}$ kcal/mol	TS Catalyst **24a**	$\Delta G^{\ddagger}$ kcal/mol	Lowering of $\Delta G^{\ddagger}$ with catalyst **24a**
spiro-*Re*-TS1	30.1	borox-*Re*-TS1	25.9	4.2
spiro-*Si*-TS1	29.8	borox-*Si*-TS1	24.1	5.7
spiro-*Re*-TS2	32.4	borox-*Re*-TS2	25.2	7.2
spiro-*Si*-TS2	31.2	borox-*Si*-TS2	27.4	3.8

We believe that this interaction is responsible for lowering the energy of borox-*Re*-TS2—enough to cause an unprecedented switch in the rate-determining step (Figure 8) of a boroxinate catalyzed aziridination reaction. Even though this interaction is absent in the (new) rate-determining step (borox-*Re*-TS1), the fact that the enantioselectivity is determined by comparing the energies of this C−C bond-forming step (borox-*Re*-TS1) to the ring-closing step in the enantiomeric pathway (borox-*Si*-TS2) accounts for why the *Re*-pathway is favored (our experimental and computational studies of related *cis*-aziridination reactions[14g] have shown that the ring-closing TS2 is inherently higher in energy than the C−C bond-forming TS1). It is noteworthy that, even though this benzhydryl CH···O interaction stabilizes borox-*Si*-TS1, it does not contribute to stabilizing the rate-determining step in the *Si*-pathway and therefore only facilitates the *Re*-pathway. Finally, careful analysis of all transition structures for the *spiro*-borate catalyst **22a** reveals that the crowding of the catalyst active site by the two BINOL ligands precludes this stabilizing benzhydryl CH···O interaction due to steric interactions between the BINOL biaryl system and the phenyl rings of the benzhydryl group. We also examined our previously published transition structures[14g] utilizing VANOL as the ligand and established that this interaction was absent even in the VANOL−boroxinate catalyst—the presence of a phenyl ring at the position

DOI: 10.1021/jacs.7b02317
J. Am. Chem. Soc. 2017, 139, 10267−10285

analogous to the 3/3′ position of BINOL precludes the benzhydryl CH···O interaction, due to steric interactions between the vaulted VANOL biaryl system and the phenyl rings of the benzhydryl/MEDAM group. One can therefore conclude that this novel interaction, that is proposed to be responsible for the observed enantiodivergence, is found only in BINOL−boroxinate systems that do not have a large substituent at the 3,3′ position—ironically, the structural feature that facilitates boroxinate formation with BINOL derivatives! It will however be interesting to examine if the boroxinate catalyst can selectively be assembled using a relatively small, electronegative substituent (−O-*t*Bu) at the 3/3′ position of BINOL that will accommodate this newly identified benzhydryl CH···O interaction at the transition state.

4. CONCLUSION

This investigation was prompted by two questions: can BINOL form a boroxinate catalyst, and why is BINOL not as effective as VANOL or VAPOL in the asymmetric catalytic aziridination reaction? Both questions have been answered. BINOL can form a boroxinate catalyst but only in a clean fashion if there are substituents in the 3- and 3′-positions. In the absence of these substituents, BINOL will react with $B(OPh)_3$ to exclusively form a *spiro*-borate anion containing two BINOL ligands per boron in the presence of an imine with either a 2:1 or 1:1 ratio of BINOL to $B(OPh)_3$. Interestingly, however, with a 1:3−4 ratio of BINOL to $B(OPh)_3$ (boroxinate formation conditions), a 2:5 mixture of the boroxinate (boroxinate **24a**) and the *spiro*-borate **22a** is formed with imine **5a**. These two species, derived from the same enantiomer of BINOL, give opposite asymmetric inductions in the aziridination reaction with ethyl diazoacetate with the net overall result that the aziridine is produced with very low optical purity (13−20% ee). A DFT analysis of the transition states for the two species reveals that the switch in the enantio-preference for the two species is a result of a switch in the rate-determining step from the ring-closing step for the *spiro*-borate **22a** to the carbon−carbon bond forming step for the boroxinate **24a**. A possible explanation can be associated with a stabilizing interaction resulting from a CH−O hydrogen bond in the ring-closing step for the boroxinate species. This interaction was not observed for the *spiro*-borate species as a result of the steric congestion associated with two BINOL ligands bonded to one boron. Similarly, this interaction is not present in transition states for the aziridination with VANOL and VAPOL boroxinate catalysts for which the ring-closing step has been shown to be the rate-limiting step.[14g]

■ ASSOCIATED CONTENT

Supporting Information

The Supporting Information is available free of charge on the ACS Publications website at DOI: 10.1021/jacs.7b02317.

PDB file for transition structure borox-*Re*-TS1 (PDB)
PDB file for transition structure borox-*Re*-TS2 (PDB)
PDB file for transition structure borox-*Si*-TS1 (PDB)
PDB file for transition structure borox-*Si*-TS2 (PDB)
PDB file for transition structure spiro-*Re*-TS1 (PDB)
PDB file for transition structure spiro-*Re*-TS2 (PDB)
PDB file for transition structure spiro-*Si*-TS1 (PDB)
PDB file for transition structure spiro-*Si*-TS2 (PDB)
PDB file for structure **22a−5a** (PDB)
PDB file for structure **22a−5b** (PDB)

Procedures for the preparation of new compounds, characterization data for all new compounds including X-data for **22a−5a** and **22a−5b**, and full details of computational investigation (PDF)

■ AUTHOR INFORMATION

Corresponding Authors

*wulff@chemistry.msu.edu
*vetticatt@binghamton.edu

ORCID

William D. Wulff: 0000-0002-5668-4312
Mathew J. Vetticatt: 0000-0001-5709-0885

Notes

The authors declare no competing financial interest.

■ ACKNOWLEDGMENTS

This work was supported by a grant from the National Institute of General Medical Sciences (GM094478). M.J.V. acknowledges funding by startup funds from the SUNY Research Foundation and XSEDE Startup Allocation # CHE140035 for access to Gaussian 09.

■ REFERENCES

(1) (a) Brunel, J. M. *Chem. Rev.* **2005**, *105*, 857−897. (b) Brunel, J. M. *Chem. Rev.* **2007**, *107*, PR1−PR45.
(2) (a) Chen, Y.; Yekta, S.; Yudin, A. K. *Chem. Rev.* **2003**, *103*, 3155−3211. (b) Akiyama, T. *Chem. Rev.* **2007**, *107*, 5744−5758. (c) Terada, M. *Synthesis* **2010**, *2010*, 1929−1982. (d) Zamfir, A.; Schenker, S.; Freund, M.; Tsogoeva, S. B. *Org. Biomol. Chem.* **2010**, *8*, 5262−5276. (e) Parmar, D.; Sugiono, E.; Raja, S.; Rueping, M. *Chem. Rev.* **2014**, *114*, 9047.
(3) Bao, J.; Wulff, W. D.; Rheingold, A. L. *J. Am. Chem. Soc.* **1993**, *115*, 3814−3815.
(4) Gao, L.; Han, J.; Lei, X. *Org. Lett.* **2016**, *18*, 360.
(5) Xue, S.; Yu, S.; Deng, Y.; Wulff, W. D. *Angew. Chem., Int. Ed.* **2001**, *40*, 2271−2774.
(6) Bolm, C.; Frison, J.-C.; Zhang, Y.; Wulff, W. D. *Synlett* **2004**, 1619−1621.
(7) Newman, C. A.; Antilla, J. C.; Chen, P.; Predeus, A. V.; Fielding, L.; Wulff, W. D. *J. Am. Chem. Soc.* **2007**, *129*, 7216−7217.
(8) Rowland, G. B.; Zhang, H.; Rowland, E. B.; Chennamadhavuni, S.; Wang, Y.; Antilla, J. C. *J. Am. Chem. Soc.* **2005**, *127*, 15696−15607.
(9) Liang, Y.; Rowland, E. B.; Rowland, G. R.; Perman, J. A.; Antilla, J. C. *Chem. Commun.* **2007**, 4477−4479.
(10) Li, G.; Liang, Y.; Antilla, J. C. *J. Am. Chem. Soc.* **2007**, *129*, 5830−5831.
(11) (a) Rowland, E. B.; Rowland, G. B.; Rivera-Otero, E.; Antilla, J. C. *J. Am. Chem. Soc.* **2007**, *129*, 12084−12085. (b) Della Sala, G.; Lattanzi, A. *Org. Lett.* **2009**, *11*, 3330−3333. (c) Larson, S. E.; Baso, J. C.; Li, G.; Antilla, J. C. *Org. Lett.* **2009**, *11*, 5186−5189. (d) Senatore, M.; Lattanzi, A.; Santoro, S.; Santi, C.; Della Sala, G. *Org. Biomol. Chem.* **2011**, *9*, 6205−6207. (e) Della Sala, G. *Tetrahedron* **2013**, *69*, 50. (f) Higuchi, K.; Suzuki, S.l; Ueda, R.; Oshima, N.; Kobayashyi, E.; Tayu, M.; Kawasaki, T. *Org. Lett.* **2015**, *17*, 154.
(12) Lou, S.; Schaus, S. E. *J. Am. Chem. Soc.* **2008**, *130*, 6922−6923.
(13) Harada, H.; Thalji, R. K.; Bergman, R. G.; Ellman, J. A. *J. Org. Chem.* **2008**, *73*, 6772−6779.
(14) (a) Zhang, Y.; Desai, A.; Lu, Z.; Hu, G.; Ding, Z.; Wulff, W. D. *Chem. - Eur. J.* **2008**, *14*, 3785−3803. (b) Zhang, Y.; Lu, Z.; Desai, A.; Wulff, W. D. *Org. Lett.* **2008**, *10*, 5429−5432. (c) Mukherjee, M.; Gupta, A. K.; Lu, Z.; Zhang, Y.; Wulff, W. D. *J. Org. Chem.* **2010**, *75*, 5643−5660. (d) Hu, G.; Gupta, A. K.; Huang, R. H.; Mukherjee, M.; Wulff, W. D. *J. Am. Chem. Soc.* **2010**, *132*, 14669−14675. (e) Wang, Z.; Li, F.; Zhao, L.; He, Q.; Chen, F.; Zheng, C. *Tetrahedron* **2011**, *67*, 9199−9203. (f) Zhao, W.; Yin, X.; Gupta, A. K.; Zhang, X.; Wulff, W.

DOI: 10.1021/jacs.7b02317
J. Am. Chem. Soc. 2017, 139, 10267−10285

D. *Synlett* **2015**, *26*, 1606. (g) Vetticatt, M. J.; Desai, A. A.; Wulff, W. D. *J. Org. Chem.* **2013**, *78*, 5142−5152.
(15) Guan, Y.; Ding, Z.; Wulff, W. D. *Chem. - Eur. J.* **2013**, *19*, 15565.
(16) Desai, A.; Wulff, W. D. *J. Am. Chem. Soc.* **2010**, *132*, 13100−13103.
(17) Zhang, Z.; Zheng, W.; Antilla, J. C. *Angew. Chem., Int. Ed.* **2011**, *50*, 1135−1138.
(18) Ren, H.; Wulff, W. D. *J. Am. Chem. Soc.* **2011**, *133*, 5656−5659.
(19) Larson, S. E.; Li, G.; Rowland, G. B.; Junge, D.; Huang, R.; Woodcock, H.; Antilla, J. C. *Org. Lett.* **2011**, *13*, 2188.
(20) Van Leeuwen, P. W. N. M.; Rivillo, D.; Raynal, M.; Freixa, Z. *J. Am. Chem. Soc.* **2011**, *133*, 18562.
(21) Zhao, W.; Huang, L.; Guan, Y.; Wulff, W. D. *Angew. Chem., Int. Ed.* **2014**, *53*, 3436−3441.
(22) Barnett, D. S.; Schaus, S. E. *Org. Lett.* **2011**, *13*, 4020.
(23) Zheng, W.; Zhang, Z.; Kaplan, M. J.; Antilla, J. C. *J. Am. Chem. Soc.* **2011**, *133*, 3339−3341.
(24) Hoffman, T. J.; Carreira, E. M. *Angew. Chem., Int. Ed.* **2011**, *50*, 10670−10674.
(25) (a) Snyder, S. A.; Thomas, S. B.; Mayer, A. C.; Breazzano, S. P. *Angew. Chem., Int. Ed.* **2012**, *51*, 4080−4084. (b) Zhang, X.; Staples, R. J.; Rheingold, A. L.; Wulff, W. D. *J. Am. Chem. Soc.* **2014**, *136*, 13971.
(26) Chen, M.-W.; Chen, Q.-A.; Duan, Y.; Ye, Z.-S.; Zhou, Y.-G. *Chem. Commun.* **2012**, *48*, 1698−1700.
(27) (a) Blay, G.; Cardona, L.; Pedro, J. R.; Sanz-Marco, A. *Chem. - Eur. J.* **2012**, *18*, 12966−12969. (b) Hardman-Baldwin, A. M.; Visco, M. D.; Wieting, J. M.; Stern, C.; Kondo, S.-I.; Mattson, A. E. *Org. Lett.* **2016**, *18*, 3766. (c) Qiu, Y.; Yang, B.; Jiang, T.; Zhu, C.; Bäckvall, J.-E. *Angew. Chem., Int. Ed.* **2017**, *56*, 3221. (d) Brioche, J.; Pike, S. J.; Tshepelevitsh, S.; Leito, I.; Morris, G. A.; Webb, S. J.; Clayden, J. *J. Am. Chem. Soc.* **2015**, *137*, 6680. (e) Das, A.; Ayad, S.; Hanson, K. *Org. Lett.* **2016**, *18*, 5416.
(28) Wipf, P.; Lyon, M. A. ARKIVOC 2007 (xii) 91−98.
(29) While the nearly identical profiles for the VANOL and VAPOL catalysts in the aziridination reaction are not completely understood at this time,[14c] some progress has been made in understanding the structure of the VANOL and VAPOL[14d] catalysts, their binding with the imine substrate,[14d] and the nature of the transition state[14g] for the reaction of the imine with the diazo compound.
(30) For a review on chiral boron acids in asymmetric catalysis including those derived from BINOL, see: Dimitrijevic, E.; Taylor, M. S. *ACS Catal.* **2013**, *3*, 945−962.
(31) (a) Hattori, K.; Yamamoto, H. *J. Org. Chem.* **1992**, *57*, 3264−3265. (b) Hattori, K.; Miyata, M.; Yamamoto, H. *J. Am. Chem. Soc.* **1993**, *115*, 1151−1152. (c) Hattori, K.; Yamamoto, H. *Tetrahedron* **1993**, *49*, 1749−1760. (d) Hattori, K.; Yamamoto, H. *Synlett* **1993**, *1993*, 129−130. (e) Hattori, K.; Yamamoto, H. *Synlett* **1993**, *1993*, 239−240. (f) Hattori, K.; Yamamoto, H. *Bioorg. Med. Chem. Lett.* **1993**, *3*, 2337−2342. (g) Hattori, K.; Yamamoto, H. *Tetrahedron* **1994**, *50*, 2785−2792. (h) Ishihara, K.; Miyata, M.; Hattori, K.; Tada, T.; Yamamoto, H. *J. Am. Chem. Soc.* **1994**, *116*, 10520−10524. (i) Lock, R.; Waldmann, H. *Tetrahedron Lett.* **1996**, *37*, 2753−2756. (j) Lock, R.; Waldmann, H. *Chem. - Eur. J.* **1997**, *3*, 143−151. (k) Banerjee, A.; Schepmann, D.; Koehler, J.; Wuerthwein, E.-U.; Wuensch, B. *Bioorg. Med. Chem.* **2010**, *18*, 7855−7887.
(32) The preparation of **13** has been called into doubt due to the failure at the preparation of related compounds. See: Chong, J. M.; Shen, L.; Taylor, N. J. *J. Am. Chem. Soc.* **2000**, *122*, 1822−1823, 10.1021/ja992922b. The involvement of **13** in heteroatom Diels−Alder reactions has been called into doubt by nonlinear effects of the ligand; see reference 37.
(33) Momiyama, N.; Tabuse, H.; Terada, M. *J. Am. Chem. Soc.* **2009**, *131*, 12882−12883.
(34) Thormeier, S.; Carboni, B.; Kaufmann, D. E. *J. Organomet. Chem.* **2002**, *657*, 136−145.
(35) Zimmer, R.; Peritz, A.; Czerwonka, R.; Schefzig, L.; Reissig, H.-U. *Eur. J. Org. Chem.* **2002**, *2002*, 3419−3428.
(36) (a) Ishihara, K.; Kuroki, Y.; Yamamoto, H. *Synlett* **1995**, *1995*, 41−42. (b) Kuroki, Y.; Ishihara, K.; Hanaki, N.; Ohara, S.; Yamamoto, H. *Bull. Chem. Soc. Jpn.* **1998**, *71*, 1221−1230.
(37) Cros, J. P.; Perez-Fuertes, Y.; Thatcher, M. J.; Arimori, S.; Bull, S. D.; James, T. D. *Tetrahedron: Asymmetry* **2003**, *14*, 1965−1968.
(38) (a) Kawate, T.; Yamada, H.; Matsumizu, M.; Nishida, A.; Nakagawa, M. *Synlett* **1997**, *1997*, 761−762. (b) Yamada, H.; Kawate, T.; Matsumizu, M.; Nishida, A.; Yamaguchi, K.; Nakagawa, M. *J. Org. Chem.* **1998**, *63*, 6348−6354.
(39) (a) Periasamy, M.; Venkatraman, L.; Sivakumar, S.; Sampathkumar, N.; Ramanathan, C. R. *J. Org. Chem.* **1999**, *64*, 7643−7645. (b) Periasamy, M.; Ramanathan, C. R.; Kumar, N. S. *Tetrahedron: Asymmetry* **1999**, *10*, 2307−2310. (c) Periasamy, M.; Kumar, N. S.; Sivakumar, S.; Rao, V. D.; Ramanathan, C. R.; Venkatraman, L. *J. Org. Chem.* **2001**, *66*, 3828−3833. (d) Liu, D.; Shan, Z.; Liu, F.; Xiao, C.; Lu, G.; Qin, J. *Helv. Chim. Acta* **2003**, *86*, 157−163.
(40) (a) Raskatov, J. A.; Thompson, A. L.; Cowley, A. R.; Claridge, T. D. W.; Brown, J. M. *Chem. Sci.* **2013**, *4*, 3140. (b) Green, S.; Nelson, A.; Warriner, S.; Whittaker, B. *J. Chem. Soc., Perkin Trans. 1* **2000**, 4403−4408. (c) Tu, T.; Maris, T.; Wuest, J. D. *Cryst. Growth Des.* **2008**, *8*, 1541−1546.
(41) Llewellyn, D. B.; Arndtsen, B. A. *Can. J. Chem.* **2003**, *81*, 1280−1284.
(42) Llewellyn, D. B.; Adamson, D.; Arndtsen, B. A. *Org. Lett.* **2000**, *2*, 4165−4168.
(43) (a) Carter, C.; Fletcher, S.; Nelson, A. *Tetrahedron: Asymmetry* **2003**, *14*, 1995−2004. (b) Chen, D.; Sundararaju, B.; Krause, R.; Klankermayer, J.; Dixneuf, P. H.; Leitner, W. *ChemCatChem* **2010**, *2*, 55−57.
(44) Martin, M.; El Hellani, A.; Yang, J.; Collin, J.; Bezzenine-Lafollee, S. *J. Org. Chem.* **2011**, *76*, 9801−9808.
(45) Kaufmann, D.; Boese, R. *Angew. Chem., Int. Ed. Engl.* **1990**, *29*, 545−546.
(46) Liu, D.-J.; Shan, Z.-X.; Wang, G.-P.; Qin, J.-G. *Wuhan Univ. J. Nat. Sci.* **2003**, *8*, 1138−1142.
(47) Shan, Z.; Xiong, Y.; Li, W.; Zhao, D. *Tetrahedron: Asymmetry* **1998**, *9*, 3985−3989.
(48) Kelly, T. R.; Whiting, A.; Chandrakumar, N. S. *J. Am. Chem. Soc.* **1986**, *108*, 3510−3512.
(49) For additional selected examples, see: (a) Wipf, P.; Jung, J.-K. *J. Org. Chem.* **2000**, *65*, 6319−6337. (b) Landells, J. S.; Larsen, D. S.; Simpson, J. *Tetrahedron Lett.* **2003**, *44*, 5193−5196. (c) Snyder, S. A.; Tang, Z.-Y.; Gupta, R. *J. Am. Chem. Soc.* **2009**, *131*, 5744−5745. (d) Qi, C.; Xiong, Y.; Eschenbrenner-Lux, V.; Cong, H.; Porco, J. A., Jr. *J. Am. Chem. Soc.* **2016**, *138*, 798.
(50) The yield was determined in a separate but identical NMR experiment ($CDCl_3$) in which an internal standard (Ph_3CH) was added after the initial spectrum was recorded. See the Supporting Information.
(51) Proper analysis and mass measurements for **14** were obtained for a material prepared from BINOL and 0.5 equiv of $B(OMe)_3$ in refluxing benzene with methanol removed with 4 Å molecular sieves in a Soxhlet extractor (ref 31h).
(52) Malkowsky, I. M.; Frölich, R.; Griesbach, U.; Pütter, H.; Waldvogel, S. R. *Eur. J. Inorg. Chem.* **2006**, *2006*, 1690−1697.
(53) Becke, A. D. J. *J. Chem. Phys.* **1993**, *98*, 5648−5652.
(54) Frisch, M. J.; Trucks, G. W.; Schlegel, H. B.; Scuseria, G. E.; Robb, M. A.; Cheeseman, J. R.; Scalmani, G.; Barone, V.; Mennucci, B.; Petersson, G. A.; Nakatsuji, H.; Caricato, M.; Li, X.; Hratchian, H. P.; Izmaylov, A. F.; Bloino, J.; Zheng, G.; Sonnenberg, J. L.; Hada, M.; Ehara, M.; Toyota, K.; Fukuda, R.; Hasegawa, J.; Ishida, M.; Nakajima, T.; Honda, Y.; Kitao, O.; Nakai, H.; Vreven, T.; Montgomery, J. A., Jr.; Peralta, J. E.; Ogliaro, F.; Bearpark, M.; Heyd, J. J.; Brothers, E.; Kudin, K. N.; Staroverov, V. N.; Kobayashi, R.; Normand, J.; Raghavachari, K.; Rendell, A.; Burant, J. C.; Iyengar, S. S.; Tomasi, J.; Cossi, M.; Rega, N.; Millam, N. J.; Klene, M.; Knox, J. E.; Cross, J. B.; Bakken, V.; Adamo, C.; Jaramillo, J.; Gomperts, R.; Stratmann, R. E.; Yazyev, O.; Austin, A. J.; Cammi, R.; Pomelli, C.; Ochterski, J. W.; Martin, R. L.;

DOI: 10.1021/jacs.7b02317
J. Am. Chem. Soc. 2017, 139, 10267−10285

Morokuma, K.; Zakrzewski, V. G.; Voth, G. A.; Salvador, P.; Dannenberg, J. J.; Dapprich, S.; Daniels, A. D.; Farkas, Ö.; Foresman, J. B.; Ortiz, J. V.; Cioslowski, J.; Fox, D. J. *Gaussian 09*, revision A.1; Gaussian, Inc.: Wallingford, CT, 2009.
(55) These exact interactions were identified as the key stabilizing interactions in analogous calculations with the VANOL ligand and using the MEDAM imine (ref 14g).
(56) Bandar, J. S.; Sauer, G. S.; Wulff, W. D.; Lambert, T. H.; Vetticatt, M. J. *J. Am. Chem. Soc.* **2014**, *136*, 10700−10707.
(57) Cannizzaro, C. E.; Houk, K. N. *J. Am. Chem. Soc.* **2002**, *124*, 7163−7169.

DOI: 10.1021/jacs.7b02317
J. Am. Chem. Soc. 2017, 139, 10267−10285